High-temperature superconductivity and related broken-symmetry states in strongly correlated electron systems

Michał Zegrodnik

Academic Centre for Materials and Nanotechnology
AGH University of Science and Technology,
Krakow, Poland

10 April 2019

Contents

1 Personal details

Name	**Michał Zegrodnik**
Employment in scientific institutions	AGH University of Science and Technology Academic Centre of Materials and Nanotechnology al. Mickiewicza 30 30-059 Krakow
Phone	+48 12 617 52 51
E-mail	michal.zegrodnik@agh.edu.pl
ORCID	0000-0001-5801-5174

2 Academic degrees

PhD in Physics	2013 AGH University of Science and Technology, Faculty of Physics and Applied Computer Science
Thesis title	**Unconventional Superconductivity in Correlated Itinerant Magnetic Systems** (cum laude)
Supervisor	Prof. dr hab. Józef Spałek
Reviewers	Prof. dr hab. Karol Wysokiński Prof. dr hab. Maciej Maśka
MSc in Technical Physics	2008 AGH University of Science and Technology, Faculty of Physics and Applied Computer Science
Thesis title	**Energy levels of Helium and Hydrogen muonic molecule determined by the use of the scattering matrix poles method**
Supervisor	Dr Wilhelm Czapliński
Reviewer	Dr hab. inż. Bartłomiej Spisak

3 Employment history in scientific institutions

since 11/2015	assistant professor Academic Centre for Materials and Nanotechnology, AGH University of Science and Technology, Krakow, Poland
11/2013 – 11/2015	research assistant Academic Centre for Materials and Nanotechnology, AGH University of Science and Technology, Krakow, Poland

4 Scientific achievements forming the basis for habilitation procedure

As a scientific achievement within the meaning of Art. 16, par. 2 of the Act of 14 March 2003 "On Academic Degrees and Academic Title and on Degrees and Title in Art" I present a series of nine related publications:

[H1] J. Spałek, M. Zegrodnik, J. Kaczmarczyk. "Universal properties of high- temperature superconductors from real-space pairing: t- J - U model and its quantitative comparison with experiment". *Phys. Rev. B* **95** (2017), 024506.

[H2] M. Zegrodnik, J. Spałek. "Universal properties of high-temperature superconductors from real-space pairing: Role of correlated hopping and intersite Coulomb interaction within the t - J - U model". *Phys. Rev. B* **96** (2017), 054511.

[H3] M. Zegrodnik, J. Spałek. "Effect of interlayer processes on the superconducting state within the t - J - U model: Full Gutzwiller wave-function solution and relation to experiment". *Phys. Rev. B* **95** (2017), 024507.

[H4] M. Zegrodnik, J. Spałek. "Stability of the coexistent superconducting-nematic phase under the presence of intersite interactions". *New J. Phys.* **20** (2018), 063015.

[H5] M. Abram M. nd Zegrodnik, J. Spałek. "Antiferromagnetism, charge density wave, and d -wave superconductivity in the extended t - J - U model: role of intersite Coulomb interaction and a critical overview of renormalized mean field theory". *J. Phys. Condens. Matter* **29** (2017), 365602.

[H6] M. Zegrodnik, J. Spałek. "Incorporation of charge- and pair-density-wave states into the one-band model of d-wave superconductivity". *Phys. Rev. B* **98** (2018), 155144.

[H7] M. Zegrodnik, A. Biborski, M. Fidrysiak, J. Spałek. "Superconductivity in the three-band model of cuprates: Variational wave function study and relation to the single-band case". *Phys. Rev. B* **99** (2019), 104511.

[H8] M. Zegrodnik, J. Spałek. "Spontaneous appearance of nonzero-momentum Cooper pairing: Possible application to the iron-pnictides". *Phys. Rev. B* **90** (2014), 174507.

[H9] M. Zegrodnik, J. Spałek. "Spontaneous Appearance of the Spin-Triplet Fulde-Ferrell-Larkin-Ovchinnikov Phase in a Two-Band Model: Possible Application to $LaFeAsO_{1-x}F_x$". *J. Supercond. Nov. Magn.* **28** (2015), 1155.

under a common title:

"**High-temperature superconductivity and related broken-symmetry states in strongly correlated electron systems**".

Discussion of results contained in the series of publications that form the basis for the habilitation application

4.1 Introduction

Theoretical description of copper-based high-temperature superconductors has been the subject of intense research for many years. The basic questions that remain without a definitive answer concern the microscopic mechanism of the formation of unconventional phases observed in the aforementioned compounds, as well as the minimal model that would allow for the reconstruction of their fundamental physical properties. The difficulties in the formulation of the appropriate theoretical approach result mainly from the fact that cuprates belong to the class of strongly correlated materials, in which the interaction energy contribution is greater than the corresponding kinetic energy part. This circumstance, which leads to complications in the formal description, at the same time, makes cuprates such an interesting family of materials with a rich phase diagram (see Fig. 1 a). It has been established, that the parent compound is an antiferromagnetic charge transfer insulator [1] with a Néel temperature ranging from 240 K to 420 K [2]. Upon doping, one can observe the creation of magnetic ordering (SDW - *spin-density wave*) and charge ordering (CDW - *charge-density wave*), as well as the superconducting phase in the doping range $\delta \lesssim 0.35$ with optimal doping $\delta \approx 0.1 - 0.2$, for which the critical temperature reaches the maximum value [3, 4, 5]. In recent years, the Cooper pair density wave state (PDW) has been reported experimentally with a modulation vector close to the one which corresponds to the periodicity of charge density wave [6]. In addition, for the temperatures above the critical temperature, the so-called pseudogap [7] phase is observed. So far, the complete unified theoretical description of the physics of copper-based materials has not been formulated. At the same time, it is not clear whether it is possible to explain the entire diversity of physical observations on the basis of a single microscopic mechanism. Due to the crucial role of Coulomb interactions in the cuprates, it seems reasonable to analyze the scenario, in which they induce superconductivity and related phenomena [8, 9, 10]. Nevertheless, it should be noted that there are alternative approaches, in which for example, antiferromagnetic spin fluctuations lead to the formation of Cooper pairs in the regime of weak correlation [11]. In addition, despite the unconventional nature of the superconducting phase in the cuprates, a scenario is also considered, in which the classical phonon-mediated mechanism plays an important role in the formation of the SC state. [12, 13, 14].

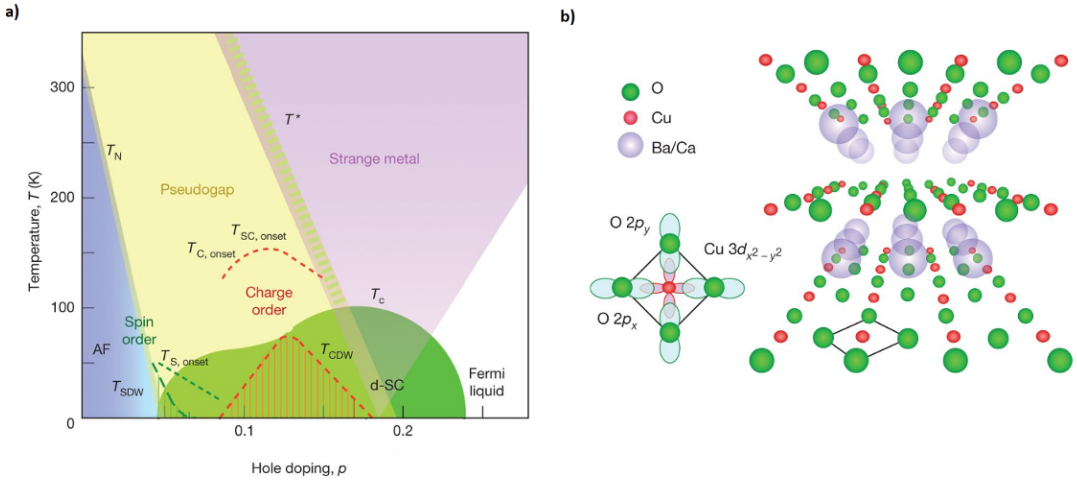

Figure 1: a) Phase diagram of copper-based high-temperature superconductors for the case of hole-doping; b) crystal structure of cuprates with visible copper-oxygen planes (red and green spheres) and a charge reservoir layer (gray spheres), which composition depends on the specific compound. Figures taken from [3].

The cuprates have a layered structure, consisting of copper-oxygen planes (1,2,3, or more in a unit cell) separated by the so-called charge reservoir with different composition, depending on the specific material (see Fig. 1 b). It is believed that the physics of copper-oxygen planes is instrumental for the unique properties of the cuprates and determines the form of their phase diagram. The high value of the Coulomb interaction integral, which corresponds to the partially filled $3d$ shells of the copper atoms suggests that the application of widely used *ab inito* methods (such as DFT) does not lead to the reproduction of basic physical properties. On the other hand, methods dedicated to correlated systems are characterized by a high degree of complexity, which limits their applicability only to simplified models and/or systems with a significantly reduced size. Therefore, a very important aspect of theoretical research is to determine the minimal model, simple enough to allow for taking into account the correlations with the appropriate accuracy. A the same time such model has to contain those degrees of freedom that are responsible for the creation of interesting phenomena.

The widely used approach is based on the effective single-band Hamiltonian for a Cu-O plane, in which the role of quasiparticles is played by the Zhang-Rice singlets [15]. One of the canonical models, within the paradigm of strong correlations, is the t-J model [16, 1], where the exchange interaction $\sim J$ appears due to projecting out these electron configurations that correspond to increased energy of the Coulomb interaction. Theoretically estimated exchange integral takes the value of $J = 0.1 - 0.16$ eV [1], which agrees well with Raman scattering measurements [17, 18, 19] as well as inelastic neutron scattering [20] for the case of parent compounds. The t-J model leads naturally to the stability of the superconducting phase already at the level of the *renormalized mean field theory* (RMFT) [21, 22]. Another model of interest in the context of copper-based superconductors is the Hubbard model [23, 24], which, however, requires more advanced computational methods in order to obtain the paired phase stability. This difference is due to the fact that in the t-J model, the pairing correlations are already included directly at the Hamiltonian level through the kinetic exchange term, whereas in the Hubbard model the correlations need be accounted for within the chosen calculation method, which requires going beyond the *renormalized mean field theory*. The approach which combines features of both models is based on the so-called t-J-U model and is analysed in detail in the series of our papers [H1, H3, H2, H5, H6]. Within such description, both the $\sim J$ term and small but non-zero number of double occupancies appear. The single-band approach was also analyzed in the context of the antiferromagnetic phase [25, 26], the spin-density-wave [27, 28, 29] and the charge-density-wave [30, 31, 32]. In addition, due to the observed relationship between the critical temperature and the number of Cu-O planes in the unit cell, the analysis of the inter-plane effects on the properties of superconducting phase has been carried out [33, 34, 35, 36, 37] .

The single-band picture of the cuprates, despite its simplicity, has led to the reconstruction of selected principal properties observed in this family of compounds. Nevertheless, it should be noted that within such approach, the oxygen degrees of freedom, are incorporated only in an effective manner. At the same time, experimental studies show that the doped holes mainly occupy the oxygen states [40]. Also, by tuning the ratio between the carriers on the copper and oxygen atoms and reducing the energy between the copper and oxygen atomic levels one can maximize the superconducting critical temperature [41, 42, 43]. These facts indicate the importance of determining how the oxygen degrees of freedom affect the physics of the cuprates. The simplest model that can be analysed in this context consists of the $3d_{x^2-y^2}$ orbital due to copper atoms, and the $2p_x$ and $2p_y$ orbitals due to oxygen atoms. As a result of the hybridization between the $2p_\sigma$ and $3d_{x^2-y^2}$ states, a partially filled antibonding band (AB) and fully filled non-bonding (NB) and bonding (B) bands are formed. After taking into account the role of the strong Coulomb repulsion, the AB band splits into upper and lower Hubbard subbands, what in turn leads to the insulating state with the gap $\approx 1 - 2$ eV for the parent compound (Fig. 2). Theoretical studies of the three-band model have shown that it is possible to reproduce the charge transfer insulating state [44, 45, 46] and the antiferromagnetic ordering appears for

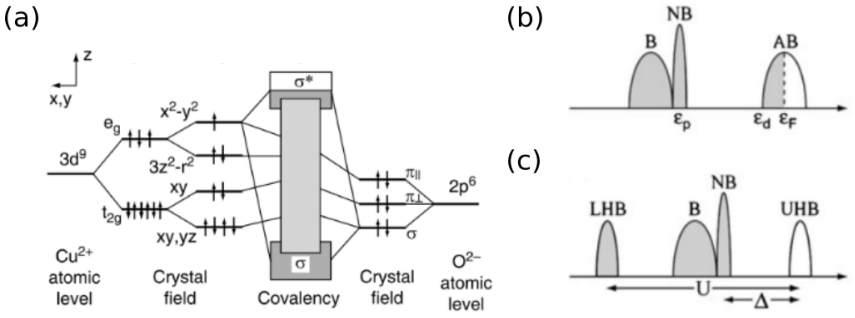

Figure 2: a) Energy level splitting for the $3d^9$ configuration due to the copper atoms and $2p^6$ due to the oxygen atoms in the Cu-O plane caused by the crystal field and the Jahn-Teller effect. Strong covalent bonds resulting from the $2p_\sigma$ and $3d_{x^2-y^2}$ states within the xy plane constitute the three-band model of the high-temperature copper-based superconductors. b) Due to the hybridization of the $2p_\sigma$ and $3d_{x^2-y^2}$ states, the anti-bonding (AB), non-bonding (NB) and bonding (B) bands are formed. c) After taking into account the role of the strong Coulomb repulsion, the AB band splits into upper and lower Hubbard subbands, which in turn lead to the insulating state with the gap $\approx 1-2$ eV. Figures taken from [38, 39].

low doping values. Moreover, the typical structure of the superconducting dome occurs for $\delta \approx 0.05 - 0.3$ [47, 48]. The similarity between the single- and three-band approaches has been highlighted in the work [49], while according to some analysis the explicit inclusion of oxygen states leads to fundamental changes in the physics of the model [50, 51].

4.2 Aim of the research

Within the research presented here, the emphasis was mainly placed on the theoretical description of the superconducting phase, as well as the antiferromagnetic and the charge density wave phases in the context of the copper-based compounds. The aim of the research was to reconstruct a number of fundamental physical properties of cuprates in the framework of a unified description based on the paradigm of strong electron correlation according to which Coulomb repulsion is the origin of the phenomena of interest. In such approach, it is important to include electron correlations with the satisfactory accuracy. For this purpose, the novel *diagrammatic expansion of the Gutzwiller wave-function* (DE-GWF) method has been extended in a essential manner allowing for a detailed analysis of selected models as well as unconventional phases. The DE-GWF-based approach allows to go beyond the widely used *renormalized mean field theory* (RMFT) in a systematic manner by including non-local correlation of the increased range in higher orders (zeroth order calculations are equivalent to RMFT). In addition, this approach is efficient from the numerical point of view and is not limited to small systems, nor is it associated with the sign problem (such restrictions are found in methods based on Monte Carlo techniques). These features allow for comprehensive studies, taking into account different variants of the models used and scanning a wide range of microscopic parameters.

First, several single-band models were analyzed to specify the one for which the fundamental experimental observations regarding the d-wave superconducting phase in the cuprates can be reproduced in the best possible manner (Sec. 4.3). Next, for the selected model, the influence of interlayer processes on the paired state is analyzed for the case of the bilayer structure (Sec. 4.4). Subsequently, the research is directed towards other broken-symmetry states, which are observed in the cuprates (Sec. 4.5). Namely, the antiferromagnetic and nematic (with possible coexistence with superconductivity) phases, as well as the charge-/pair-density wave phase. This allowed to create a fairly complete phase diagram for the copper-based compounds within the single-band approach, in which the symmetry-braking for particular states is induced by the collective

phenomena described within the strong Coulomb interaction paradigm. In addition, due to the mentioned limitations of the single-band approach, the analysis has been extended to the case of the three-band model, in which the oxygen degrees of freedom are included explicitly. In this manner the DE-GWF method has been applied for the first time to the multiband description of superconductivity. The obtained results were analyzed in the context of experimental data for the cuprates, and the two approaches in use (single- and three-band description) have been compared (Sec. 4.6).

The presented research on unconventional superconductivity has also led to proposing an unconventional Fulde-Ferrell-Larkin-Ovchinnikov-type (FFLO) paired phase, which may occur spontaneously, i.e. without the application of any external field. A prerequisite for the stability of such phase is the presence of an inter-band pairing channel and an appropriate mismatch between the two Fermi surface sheets between which the pairing occurs. Due to the multiband character of the superconducting state that is observed in the family of iron-based compounds [52], the proposed idea has been tested with the use of a model appropriate for those systems. The iron-based materials in many aspects resemble the cuprates. Namely, superconductivity also stabilizes due to doping of the parent compound, and for relatively low doping levels the system is magnetically ordered. Nevertheless, iron-based compounds are considered to be less correlated than the cuprates and have a different gap symmetry. The purpose of such analysis was to verify whether the band structure of the selected compound allows for the appearance of stable FFLO state of the proposed type. One of the interesting features of this concept is the possibility of obtaining a material in which the superconducting current flows in the absence of an external factor in the form of a magnetic or electric field. The results of the analysis are described in the Sec. 4.7.

4.3 High-temperature superconductivity in the effective single-band approach (papers [H1, H2])

In this Section we present a detailed analysis of the fundamental properties of the superconducting state by applying different variants of the single-band approach to the description of Cu-O planes with a quantitative comparison to experiment (papers [H1, H2]). The purpose of this study is to specify the single-band model which is best suited to describe the superconducting phase by comparing the theoretical results with the available experimental data.

First, the Hubbard, t-J, and t-J-U models have been analyzed (paper [H1]). The general form of Hamiltonian, which in different variants corresponds to the three models, is presented below.

$$\hat{\mathcal{H}} = \sum_{\langle ij\rangle\sigma}{}' t_{ij}\hat{c}^{\dagger}_{i\sigma}\hat{c}_{j\sigma} + U\sum_{i}\hat{n}_{i\uparrow}\hat{n}_{i\downarrow} + \sum_{\langle\langle ij\rangle\rangle}{}' J_{ij}\hat{\mathbf{S}}_i\cdot\hat{\mathbf{S}}_j, \tag{1}$$

where $\hat{c}^{\dagger}_{i\sigma}$ ($\hat{c}_{i\sigma}$) are the creation (annihilation) operators of particles in an effective single-band. The primmed summation is with the restrictions $i \neq j$, while $\langle i,j\rangle$ and $\langle\langle i,j\rangle\rangle$ refer to the nearest- and next nearest-neighbors, with the hopping integrals $t = -0.35$ eV and $t' = 0.25|t|$, respectively. The first two terms represent kinetic (hopping) part and strong onsite Coulomb repulsion, respectively, while the third term corresponds to the antiferromagnetic kinetic exchange. Such Hamiltonian defines the so-called t-J-U model. For the case of $J = 0$ we obtain the Hubbard model, while in the limit of zero double occupancies, $d_G^2 \to 0$ ($U \to \infty$) we arrive at the t-J model [16, 53]. In order to take into account the electronic correlations induced by the large value of Coulomb repulsion ($U >> |t|$) with a satisfactory accuracy, the method of diagrammatic expansion of the Gutzwiller wave function (DE-GWF) was used. Within such approach the correlations with increased range are accounted for in higher orders of our expansion. For comparison, in selected cases, the calculations were also carried out based on the zeroth order expansion, which is equivalent to RMFT. In the presented results, all the energies are given in units of $|t|$.

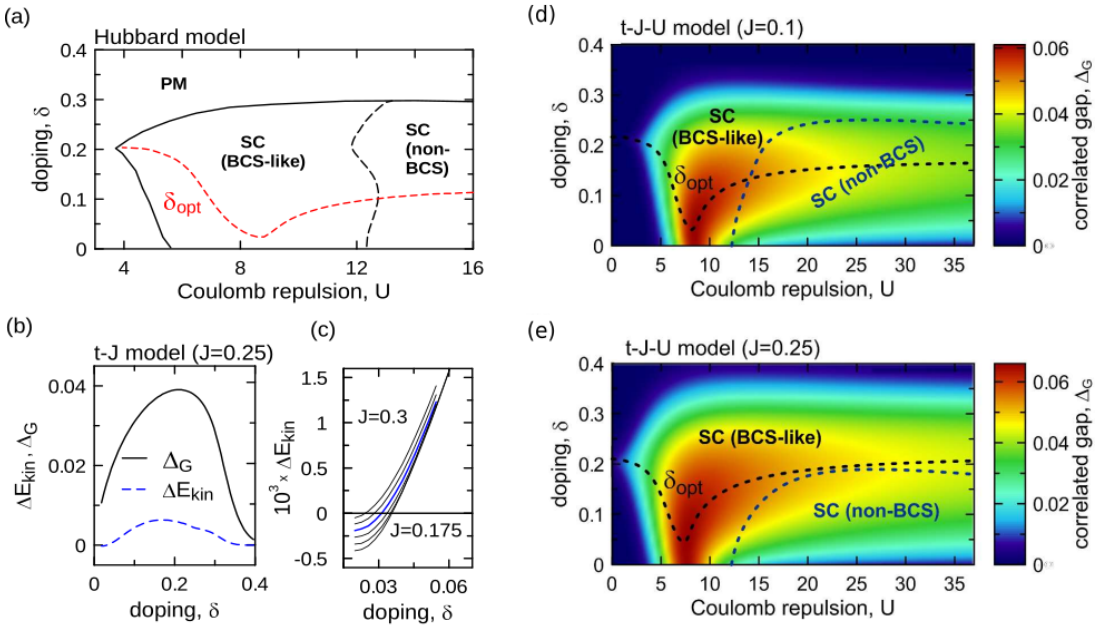

Figure 3: (a) Phase diagram in the (δ, U) plane obtained for the case of the Hubbard model with visible regions of stability of the superconducting (SC) and paramagnetic (PM) phases; (b,c) Amplitude of the correlated superconducting gap (Δ_G) and kinetic energy gain at the transition to the SC state (ΔE_G) for the t-J model, for selected values of J; (d,e) Phase diagrams for the t-J-U model for two selected values of J. In Figs. (a,d,e) the values of dopings, which correspond to the maximum superconducting amplitude (optimal doping- $\delta_{\rm opt}$) are marked. For the case of the t-J-U model with $J = 0.25$ the non-BCS superconducting phase for which $\Delta E_{\rm kin} < 0$ appears in the area $\delta < \delta_{\rm opt}$ which is in agreement with the experimental observations (e). Figures taken from [H1].

The DE-GWF method was used to determine the phase diagrams in (U, δ) plane, for the principal single-band models (Fig. 3). The obtained theoretical results were first verified based on available experimental data corresponding to the superconducting phase stability range, optimal doping values ($\delta_{\rm opt}$) and the appearance of the non-BCS and BCS-like regimes. The two last are characterized by the negative and positive values of the kinetic energy gain at the transition to the SC state, respectively. The kinetic energy gain is defined as follows

$$\Delta E_{\rm kin} \equiv E^{SC}_{G|0} - E^{PM}_{G|0}, \quad E_{G|0} \equiv \frac{1}{N} \sum_{ij\sigma}{}' t_{ij} \langle \hat{c}^{\dagger}_{i\sigma} \hat{c}_{j\sigma} \rangle_G, \tag{2}$$

where $E^{SC}_{G|0}$ and $E^{PM}_{G|0}$ are the kinetic energy contributions to the total energy in the superconducting and paramagnetic states, respectively. As determined by the measurements of optical conductivity for the cuprates [54, 55, 56], the transition between the two regimes takes place near the optimal doping, with the non-BCS behavior ($\Delta E_{\rm kin} < 0$) appearing in the underdoped region ($\delta < \delta_{\rm opt}$). As can be seen from Fig. 3, in the strong correlations regime ($U \gtrsim 10$) all three models lead to the stability of the superconducting phase in the range of dopings $\delta \lesssim 0.35$, with optimal doping $\delta_{\rm opt} \approx 0.1 - 0.2$, corresponding to the maximum value of correlated gap. Such a result agrees quite well with the experimental result [4, 1]. However, discrepancies appear when it comes to the presence of the non-BCS and BCS-like regimes. Namely, both Hubbard (a) and t-J models (b, c) do not lead to the transition between the two regimes for doping levels close to $\delta_{\rm opt}$. However, such transition is obtained for the t-J-U model for a relatively large value of U ($U \gtrsim 20$) and $J \approx 0.25$ (e). It should be noted that these values are close to those resulting from previous estimates for Coulomb repulsion and the exchange integral between the

copper atoms in the Cu-O plane [57, 58, 59, 1]. As shown in Fig. 4 (a), for the two selected sets of parameters the values of $\Delta E_{\rm kin}$ calculated within the t-J-U model, agree very well with the available experimental data [54]. It should be noted, that the same model does not lead to similar agreement for the case of zeroth order expansion calculations. This indicates that the role of the higher-order terms of our diagrammatic expansion is significant in reconstructing the experimental picture of the SC phase in the cuprates.

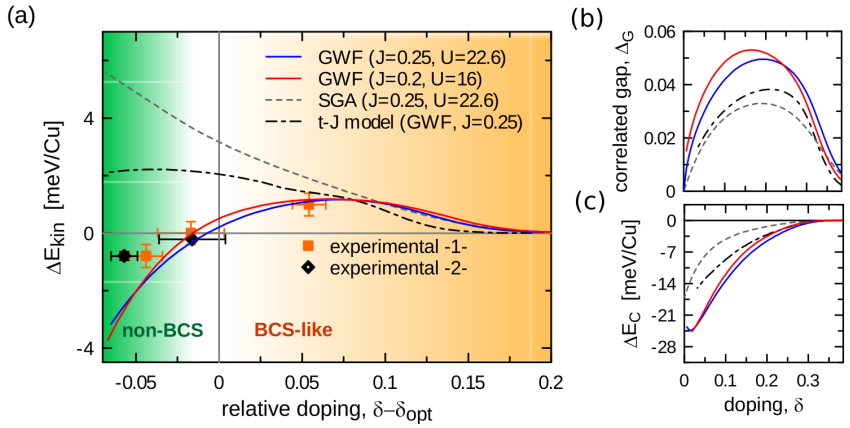

Figure 4: (a) Kinetic energy gain at the transition to the SC phase for two sets of the t-J-U model parameters (blue and red curves). The experimental data was taken from Ref. [54]. For comparison, the results obtained within the zeroth order expansion for the t-J-U model (gray dashed curve for the SGA method, which is an RMFT modification) and for the t-J model in higher orders (black dashed-dotted curve), were also plotted; (b, c) Correlated superconducting gap and the condensation energy for the same parameters and models as plotted in (a). Good agreement with experimental data was obtained only for the t-J-U model with the inclusion of the higher order terms of the diagrammatic expansion. Figures taken from [H1].

Another characteristic feature of the cuprates is the very weak doping dependence of the nodal Fermi velocity and effective mass [60, 61, 62, 63]. Direct comparison of the theoretical results with available experimental data is presented in Fig. 5. Similarly as in the previous case, the best agreement is obtained for the t-J-U model with the same values of parameters as in Fig. 4. Additionally, the calculated values of the Fermi momentum as a function of doping agree relatively well with the experiment [Fig. 5 (c)]. It should be noted that in the overdoped regime, where electron correlations become weaker due to the large number of holes in the system, both the RMFT and DE-GWF approaches give similar results.

The analysis of the three principal single-band models as applied to the description of the cuprates shows that the best agreement with the experiment is obtained for the t-J-U model, with the inclusion of the higher order terms of the diagrammatic expansion. Nevertheless, within such an approach, some of the two-site terms were neglected, which potentially may lead to different physical behavior of our system. Therefore, in the subsequent stage of the research, the influence of principal two-site interaction terms, is analyzed (paper [H3]). Namely, in the t-J-U Hamiltonian considered earlier, the correlated electron hopping and the intersite Coulomb repulsion were additionally taken into account. The explicit form of those two is provided below.

$$\hat{H}_K = \sum_{\langle ij\rangle\sigma} K(\hat{n}_{i\bar{\sigma}} + \hat{n}_{j\bar{\sigma}})\hat{c}^{\dagger}_{i\sigma}\hat{c}_{j\sigma}, \quad \hat{H}_V = V\sum_{\langle ij\rangle}\hat{n}_i\hat{n}_j. \tag{3}$$

The first results from the off-diagonal matrix elements of the Coulomb repulsion between the nearest-neighbors, and the corresponding interaction integral is $K_{ij} = \langle \mathbf{ii}|V(\mathbf{r}-\mathbf{r}')|\mathbf{ij}\rangle$. As it has been shown in earlier studies, such term may lead to the stability of the superconducting state already at the level of the mean field theory [64, 65]. On the other hand, it is expected that the second term ($V_{ij} = \langle \mathbf{ij}|V(\mathbf{r}-\mathbf{r}')|\mathbf{ij}\rangle > 0$) has a negative effect on superconductivity as

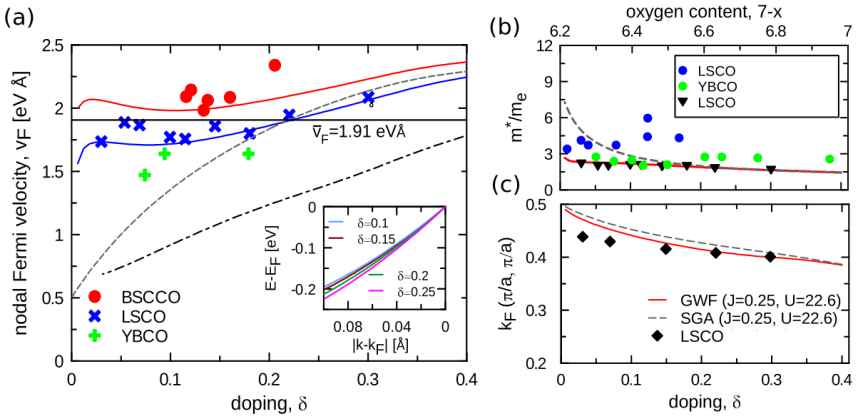

Figure 5: Nodal Fermi velocity (a) relative effective mass (b) and Fermi momentum (c) as functions of doping calculated for the same parameters and models as in Fig. 4 (colors of the curves are also the same). Very good agreement with the experiment was obtained for the t-J-U model within the DE-GWF approach. The experimental data were taken from [62, 63, 60, 61, 4]. Additionally, the inset in (a) shows the calculated dispersion relation near the nodal point. Figures taken from [H1].

it increases the energy associated with the configuration corresponding to the intersite Cooper pair. At this stage the doping range within which the analysis is carried out is extended to the electron-doping side of the phase diagram ($\delta < 0$).

As can be seen in Fig. 6, for the t-J-U model supplemented with the terms (3), at the electron-doped side the superconductivity is weaker (the correlated gap has lower values) and appears in a narrower doping range, what reproduces qualitatively the experimental situation [39]. Correlated hopping broadens the area of superconducting phase stability mainly on the electron-doped side and slightly shifts the doping corresponding to the transition between the non-BCS and BCS-like regimes towards $\delta = 0$. As it has been expected, the intersite Coulomb repulsion, negatively affects the superconductivity by decreasing the value of the upper critical doping. In general, the calculations show that both correlated hopping and intersite Coulomb repulsion have no major effect on the physical picture of superconductivity in a single-band approach, for $K \lesssim 0.2$ and $V < 1.0$, respectively. In addition, in this parameter range the reduction of the upper critical doping caused by the presence of the $\sim V$ term improves the agreement with the experimental value, without affecting other theoretically reproduced features. It should be mentioned that the calculations for the case of the Hubbard model, extended by the correlated hopping term, showed an unusual behavior of the correlated superconducting gap as a function of doping (cf. Fig. 6 from Ref. [H2]), with the possibility of phase separation appearance, which is not reported in the experimental situation.

The features of the quasi-particle dispersion relation were determined for the case of the extended model for both the electron and hole dopings with $K \neq 0$. The influence of correlated hopping on the value of chemical potential and Fermi momentum is small. The comparison of the theoretical values of the Fermi momenta with the experimental corespondents have already been shown in Fig. 5 for the case of hole doping. For the case of electron doping the theoretical results agree quite well with the few available experimental points [66, 67]. Measured values of the chemical potential shift in LSCO [4] also agree well with the theory in the doping range $\delta > \delta_{\rm opt} \approx 0.2$. For $\delta < \delta_{\rm opt}$ the discrepancies are more visible. As the K parameter increases, the Fermi velocity in the nodal direction decreases. Nevertheless, the calculated values still remain within the limits set by the available experimental data [66, 67]. Particularly, for $K \lesssim 0.35$ the weak dependence of v_F on doping is preserved.

To summarize, the results presented in this Section show that among the analyzed single-band models, the one that leads to the best agreement with the experiment is the t-J-U model. In

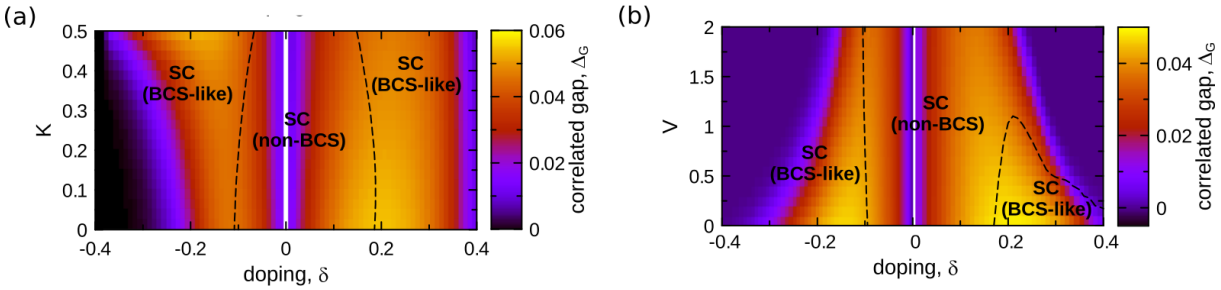

Figure 6: Correlated superconducting gap as a function of doping and correlated hopping integral (a), as well as intersite Coulomb repulsion integral (b), for the t-J-U model with parameters $U = 21$ and $J = 0.25$. Correlated hopping does not affect the physical picture of the superconducting state in the range $K \lesssim 0.2 - 0.3$ (a), while the intersite Coulomb repulsion negatively influences superconductivity by reducing the upper critical doping for SC phase formation (b). Figures taken from [H2].

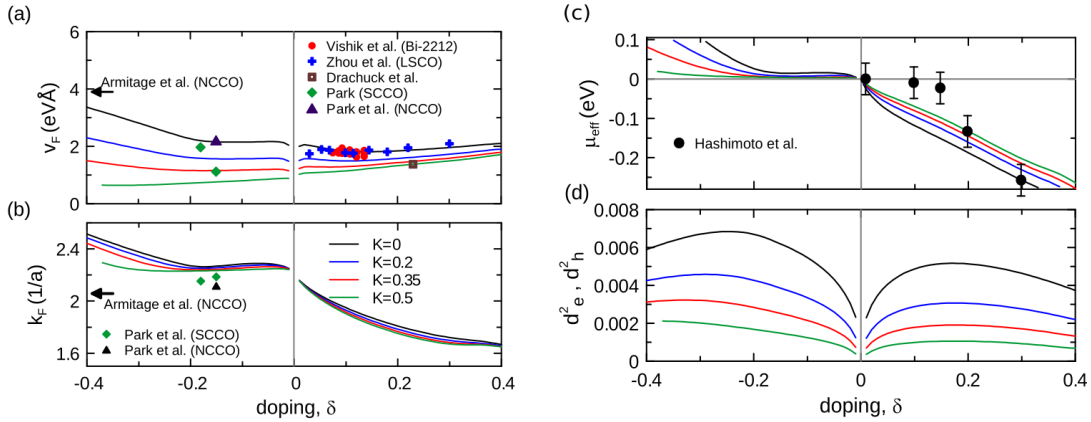

Figure 7: Nodal Fermi velocity (a), Fermi momentum (b), chemical potential (c), as well as the double occupancies of holes and electrons (d) as functions of doping for the t-J-U model ($U = 21$, $J = 0.25$) supplemented with the correlated hopping term for selected values of the K parameter. Experimental data were taken from [66, 67, 68, 62, 69, 4]. Figures taken from [H3].

combination with the DE-GWF method, it allows to reproduce the principal universal properties of the superconducting state in copper-based compounds. Namely, (*i*) the calculated correlated pairing amplitude reflects the dome-like structure of the superconducting phase, with the upper critical doping $\sim 0.35 - 0.4$ and optimal doping $\sim 0.1 - 0.2$, which agrees quite well with the experimental picture; (*ii*) the asymmetry between the superconducting stability regions for the electron- and hole-dopings has been obtained, in favor of the latter, similarly as in the family of copper-based compounds; (*iii*) the transition between the non-BCS and BCS-like regimes has been obtained close to the optimal doping, with the non-BCS behavior contained in the underdoped regime - quantitative agreement with experiment for $\Delta E_{\rm kin}(\delta)$; (*iv*) calculated nodal Fermi velocity, Fermi momentum and effective mass are weakly doping dependent and agree quantitatively with the available experimental data.

It should be noted that the agreement in all of the above aspects appears for a single set of model parameters. Namely, the electron hopping integrals have typical values for the cuprates and are similar to those determined in the previous studies carried out with the use of *ab initio* calculations and by fitting the Fermi surface topology to the experimental situation [1]. Within the presented approach, the term $\sim J$ is due to the superexchange between the copper d-orbitals via the antibonding $2p_\sigma$ states due to oxygen. According to previous study carried out with

the use of cluster calculations the value of $J = 0.1 - 0.13$ eV, while the calculated Coulomb repulsion integral at the d orbitals takes the value $U = 7 - 10$ eV. Both values are similar to those for which we have obtained agreement within the t-J-U model ($J = 0.09$ eV and $U = 8$ eV). Equally important, the obtained physical picture of the superconducting state is preserved for the extended model supplemented with the two-site terms (correlated hopping and intersite Coulomb repulsion). Therefore the necessary components of the theoretical description are already included at the level of pure t-J-U model. Two principal features that characterize the presented approach are the presence of the antiferromagnetic exchange interaction term (it also occurs in the t-J model) and small but non-zero double occupancies (appears also in the Hubbard model). For the value of $U \sim 8$ eV and $d^2 \sim 10^{-2}$ we obtain the energy contribution from the Coulomb term $Ud^2 \lesssim 80$ meV, with the value $J \sim 100$ meV and the kinetic energy $4|t| \approx 140$ meV for $\delta = 0.1$ (around the optimal doping). From this estimation it can be seen that for non-zero dopings the model situation corresponds to a truly correlated state in which each of the three factors play a significant role. From the interplay between all three, and taking into account electron correlation in higher orders of diagrammatic expansion, the unconventional character of the superconducting state emerges which leads to the reproduction of the principal experimental observations.

4.4 Effect of the interlayer processes on the superconducting phase characteristics (paper [H3])

According to the results presented in the previous Section, the t-J-U model leads to a good agreement with the principal experimental observations corresponding to the superconducting phase of the cuprates. Nevertheless, these studies were limited to the description of a single Cu-O plane. In the family of the copper-based compounds there are systems, which have more than one copper-oxygen plane in the unit cell, and the critical temperature is proportional to the number of planes for $n \leq 3$ [70]. Therefore, at the next stage of the research, a structure consisting of two Cu-O layers has been considered and the influence of the inter-layer processes on superconductivity has been analyzed. The intra-layer part of the Hamiltonian, is determined by the t-J-U model given by Eq. (1), whereas the inter-layer part is shown below

$$\begin{aligned}\hat{\mathcal{H}}_{\perp} =& \sum_{ijll'\sigma}{}'' t_{ij}^{\perp} \hat{c}_{il\sigma}^{\dagger} \hat{c}_{jl'\sigma} + \sum_{ijll'}{}'' J_{ij}^{\perp} \hat{\mathbf{S}}_{il} \cdot \hat{\mathbf{S}}_{jl'} + U'' \sum_{ijll'}{}'' \left(\hat{c}_{il\uparrow}^{\dagger} \hat{c}_{jl\downarrow}^{\dagger} \hat{c}_{jl'\downarrow} \hat{c}_{il'\uparrow} + \hat{c}_{il\uparrow}^{\dagger} \hat{c}_{jl\downarrow}^{\dagger} \hat{c}_{il'\downarrow} \hat{c}_{jl'\uparrow} \right) \\ &+ U' \sum_{ill'}{}'' \hat{c}_{il\uparrow}^{\dagger} \hat{c}_{il\downarrow}^{\dagger} \hat{c}_{il'\downarrow} \hat{c}_{il'\uparrow},\end{aligned} \tag{4}$$

where l, l' enumerate the two Cu-O layers ($l = 1, 2$), and double-primed sums are limited to $i \neq j$, $l \neq l'$. The subsequent terms represent the electron hopping between the layers, the inter-layer exchange interaction, as well as the pair-hopping of electrons between the layers.

The interlayer hopping term leads to the Fermi surface splitting into bonding and anti-bonding sheets. The values of the hopping parameters are selected so that the single-particle part in the reciprocal space has the form [71]

$$\mathcal{H}_{\perp}^{t} = \sum_{\mathbf{k}ll'\sigma}{}'' \left[t_{\mathrm{bs}} + \frac{t_z}{4} (\cos k_x - \cos k_y)^2 \right] \hat{c}_{\mathbf{k}l\sigma}^{\dagger} \hat{c}_{\mathbf{k}l'\sigma} \ , \tag{5}$$

where t_{bs} and t_z correspond to the isotropic and anisotropic part of the Fermi surface splitting, respectively. The latter determines the splitting in the antinodal direction, and the former in the nodal direction. It is very difficult to carry out the diagrammatic expansion in higher orders for the case of the four-site $\sim U''$ term. Therefore, this particular term has been included in the calculations within the zeroth order expansion. This is justified by the fact that the value of U'' is much smaller than U.

In the considered situation, apart from the intra-layer pairing, one should also take into account the inter-layer contribution, which can lead to deviations from pure *d-wave* symmetry. Such deviations are observed in some of the experiments for the cuprates [72, 73] and they can influence the stability of the superconducting phase, as well as modify the critical temperature. In this study, the intra-layer *d-wave* pairing with an admixture of interlayer $s^{\pm}$ symmetry has been considered. The correlated superconducting gap in the reciprocal space takes the form

$$\Delta_G(\mathbf{k}) = 2\Delta_G^{||}(\cos k_x + \cos k_y) \pm \Delta_G^{\perp}, \tag{6}$$

where $\pm$ corresponds to the bonding and antibonding Fermi surface sheets while $\Delta_G^{||}$ ($\Delta_G^{\perp}$) is the intralayer (interlayer) pairing amplitude in the correlated state.

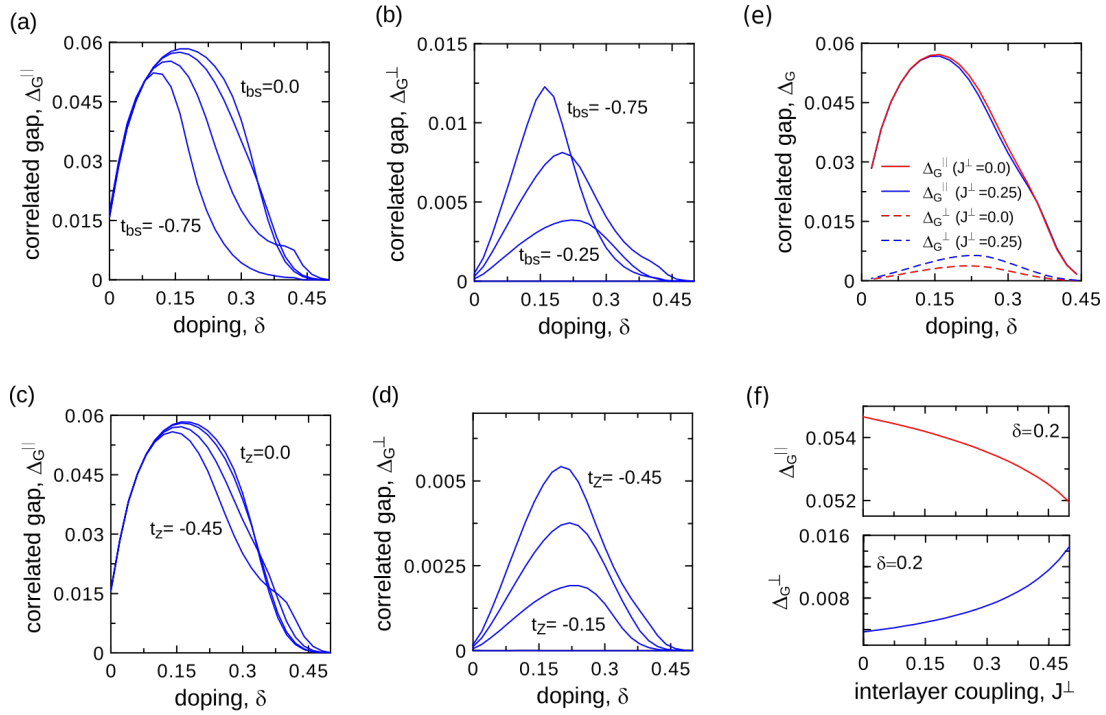

Figure 8: Intra-layer (a,c) and inter-layer (b,d) correlated gaps as a function of doping for selected values of inter-layer isotropic ($t_{\rm bs}$) and anisotropic (t_z) hopping amplitudes for $J^{\perp} = 0$, $U' = U'' = 0$; (e) $\Delta_G^{\perp}$ and $\Delta_G^{||}$ as a function of doping for $t_z = -0.3$, $t_{\rm bs} = 0$, for selected values of $J^{\perp}$; (f) $\Delta_G^{\perp}$ and $\Delta_G^{||}$ as a function of $J^{\perp}$ for selected doping value close to the optimal doping, $\delta = 0.2$. Figures taken from [H3].

According to our analysis, the non-zero values of $\Delta_G^{\perp}$ appear already for case with $J^{\perp} = 0$, $U' = U'' = 0$, $t_{\rm bs} \neq 0$, $t_z \neq 0$ (Fig. 8 a, b, c, d). Thus, inter-layer hopping is enough to induce inter-layer pairing in the system. However, this effect does not appear in the zeroth order calculations (RMFT). This again shows the importance of the higher orders terms of diagrammatic expansion for the creation of the superconducting phase. The amplitude of the inter-layer pairing is one order of magnitude smaller than its intra-layer corespondent (Fig. 8), and the maxima of both components of the pairing appear for similar doping values, so $\Delta^{\perp}$ should not have significant influence on the superconducting dome structure observed in the cuprates.

Both anisotropic and isotropic Fermi surface splitting have similar effect on pairing amplitudes, increasing $\Delta_G^{\perp}$ and slightly decreasing $\Delta_G^{||}$, mainly in the overdoped region $\delta > \delta_{\rm opt}$. Nevertheless, the overall behavior of $\Delta_G^{||}$ as a function of doping is similar to that corresponding to the single-layer structure (see Fig. 8 a, c and 4 b). The influence of inter-layer pairing in the realistic range of $J^{\perp}$ value also does not influence the intra-layer pairing significantly (Fig.

8 e, f). As expected, with increasing $J^{\perp}$, $\Delta^{\perp}$ also increases. Nevertheless, the latter still has relatively small values.

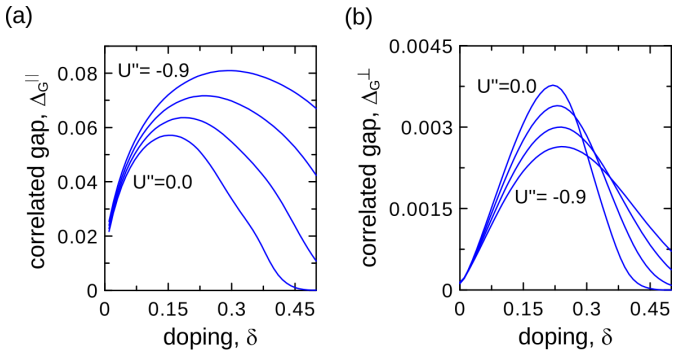

Figure 9: Intralayer (a) and interlayer (b) superconducting gap as a function of doping for $t_{\rm bs} = 0$, $t_z = -0.3$, $J^{\perp} = 0$, and for selected values of U' ranging from 0.0 to -0.9 with a step of 0.3 assuming $U' = -2U''$. Figures taken from [H3].

In contrast to the processes analyzed above, the inter-layer tunneling of the Cooper pairs has a significant influence on the stability of the superconducting phase. As one can see in Fig. 9, with increasing $|U"|$ the stability region of the superconducting phase widens and the maximum value of the intralayer pairing amplitude increases. The effect is strong even though the selected values of $U"$ are small in relation to the chosen values of U. Thus, within such description, the increase of the critical temperature value for materials with more than one Cu-O plane in the unit cell, should be mainly due to the inter-layer tunneling of the Cooper pairs.

In the next stage of the research, the model parameters were chosen so as to obtain agreement with the basic characteristics measured by electron spectroscopy for the superconducting state in the bi-layer compound Bi-2212 [60]. As can be seen from Fig. 10 (a), the Fermi surface splitting is strongly anisotropic, just like in experiments [60]. The nodal splitting value in the overdoped regime agrees well with the measured values. For dopings below $\delta_{\rm opt}$, the calculated value $\Delta_{\rm BS}$ decreases significantly below the level corresponding to the measured values. However, there are experimental reports of a total drop in $\Delta_{\rm BS}$ below the optimal doping [74]. This discrepancy between different sets of experimental results [60, 61, 74] on the one hand and theoretical results on the other, requires further analysis. The calculated Fermi velocity values are close to those measured experimentally and are ≈ 2 eV Å for both the bonding and antibonding Fermi surface sheets. Unfortunately, to the best of our knowledge, there are no available measurements that would distinguish between two Fermi velocities, therefore it is impossible to directly compare the theoretical values with experiment for both of them. Good agreement has also been obtained when it comes to comparing the dispersion relation near Fermi energy for the selected doping value (Fig. 10c).

To summarize, the research on the copper-oxide bilayer structure indicates that the basic properties of the superconducting state, obtained within the description based on a single-band model t-J-U, do not change fundamentally as a result of interlayer effects. However, in systems with larger number of layers, the increase of the critical temperature is mainly caused by the interlayer hopping of pairs. In addition, for the bilayer model, it was possible to obtain quite good agreement between the theoretical and experimental results for the Bi-2212 compound (see Fig. 10).

4.5 Charge-density-wave, nematicity, and antiferromagnetic phase in single-band models of the cuprates (papers [H4, H5, H6])

In previous sections the principal research results, corresponding to the pure superconducting phase, have been presented. In this Section, the analysis is extended for the case of the remaining

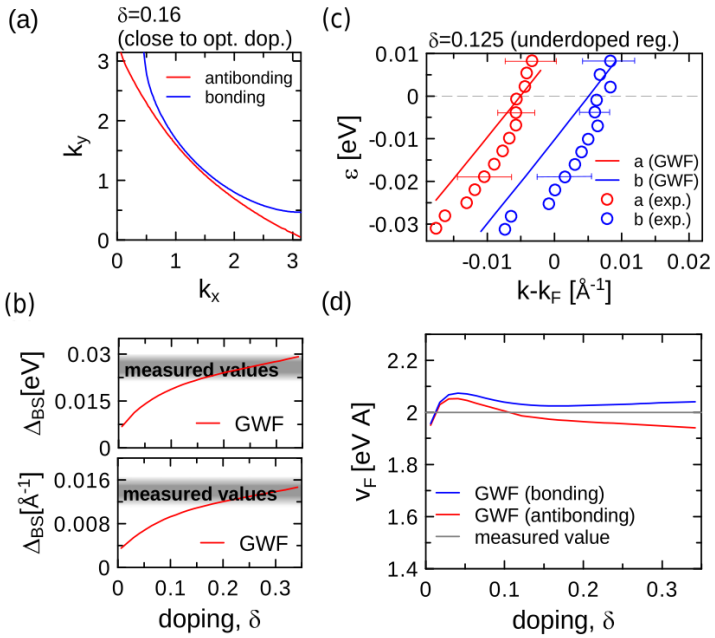

Figure 10: (a) Fermi surface sheets for selected doping value near the optimal doping; (b) Bilayer splitting in the nodal direction as a function of doping. Gray areas represent values measured experimentally [60]; (c) theoretical (lines) and experimental [60] (circles) dispersion relations as a function of doping; (d) Fermi's nodal velocity corresponding to the bonding and anti-bonding band as a function of doping. The presented results were obtained for the parameters $t' = 0.36$, $t_z = -0.15$, $t_{\rm bs} = -0.06$, $U = 13.5$, and $J = 0.25$. Figures taken from [H3].

unconventional states with broken symmetry that are observed in the cuprates. Moreover, in selected cases the possibility of their co-existence with the superconductivity will be analyzed.

At first the nematic ordering with possible coexistence with superconductivity is going to be analyzed. Nematicity is characterized by a spontaneous rotational symmetry breaking with preservation of the translational symmetry corresponding to the crystal lattice. Since there is a small rhombohedral distortion in some of the compounds from the cuprate family, it is not easy to identify the nematicity due to the fact that the C_4 symmetry is already broken by the crystal lattice itself. Nevertheless, despite a very small distortion, there is a relatively large anisotropy of various physical quantities [75, 76, 77]. This indicates that anisotropy in copper-based compounds is not a trivial consequence of the distortion of the lattice, instead it comes as a result of the susceptibilty of the electronic wave function towards a spontaneous C_4 symmetry breaking, which can be induced by electron correlations [78, 79]. The latter hypothesis is analyzed in the paper [H4] within a single-band approach using the DE-GWF method. Additionally, it is believed that the nematic state may be considered as a kind of a precursor state before the formation of the CDW state [78]. This makes the nematicity an interesting subject from the perspective of the whole phase diagram of the cuprates.

The calculations for the Hubbard model are presented in Fig. 11 with typical values of the hoppingu parameters $t = -0.35$ eV and $t' = 0.25|t|$. As can be seen spontaneous C_4 symmetry breaking appears in a relatively large area of the phase diagram, wherein the nematic phase order parameter is $\delta P_G = P^G_{1,0} - P^G_{0,1} \neq 0$, with $P^G_{X,Y} = \langle \hat{c}^\dagger_{i\sigma} \hat{c}_{j\sigma} \rangle_G$ [cf. Fig. 11 (c)]. The nematic phase coexist with superconductivity, which in this case has a mixed gap symmetry [*s-wave* (a) + *d-wave* (b)]. The amplitude of the *s-wave* component is two orders of magnitude smaller than the *d-wave* corespondent and it is induced by the C_4 symmetry braking. The situation for which the nematic phase has not been included in the calculations is presented in Fig. 11 (d). From comparison between Fig. 11 (b) and (d) one can see that the nematicity relatively strongly

negatively affects the *d-wave* superconductivity. This points to the competition between the two phases (SC and N), which, however, is not strong enough for one of the phases to completely dominate the other. This allows for the appearance of a significant coexistence region.

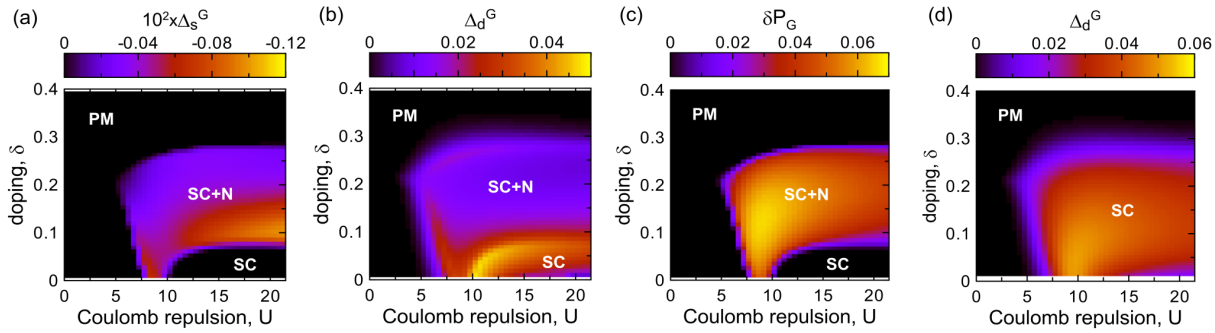

Figure 11: Pairing amplitudes corresponding to *s-wave* (a) and *d-wave* (b) symmetries, as well as the nematic phase order parameter (c) as a function both doping and Coulumb repulsion integral. Additionally, in (d) the diagram with no nematicity included is presented (only the *d-wave* superconductivity). Figures taken from [H4].

As follows from the analysis, the competition between the SC and N phases is strongly influenced by two terms appearing in extended versions of single-band Hamiltonian, which in this respect have the opposite effect. Namely, as it turned out, the $\sim J$ term promotes the superconducting phase at the expense of the nematic phase. Figures 12 (a), (b) and (c) show that the nematic phase stability region is decreased, in favor of the pure *d*-wave SC state, with increasing J value. In particular, for a set of model parameters (in this case the *t-J-U* model) for which good agreement between theory and experiment was obtained with regard to the pure superconducting phase (see chapter 4.3), the nematicity is completely removed from the phase diagram. An opposite effect is obtained for the case of the intersite Coulomb repulsion [cf. Fig. 12 (d), (e) and (f)], which promotes the nematic phase at the expense of superconductivity. As a result, for significant values of the V parameter the nematicity may still occur in the *t-J-U-V* model (see Fig. 5 from the work [H4]).

The influence of the so-called correlated electron hopping term on the discussed phenomena is not significant in the range reaching relatively large values of the K parameter ($K \lesssim 1$) (see Fig. 6 in [H4]). For the sake of completeness, calculations were also carried out for various forms of the electronic structure, characterized by the t' parameter (Fig. 4 (b), (d), (f) in [H4]). The value of t' may differ slightly for various compounds from the copper family. With decreasing t', the upper critical doping for the appearance of nematicity decreases, while the overall picture of the nematic and superconducting phases in the considered models does not change.

It should be noted that in the present analysis a square lattice without any rhombohedral distortion has been considered. This means that the observed effects of the nematic phase formation, as well as its coexistence with superconductivity, have a spontaneous character and result from strong electron correlations induced by the Coulomb repulsion. Similarly as in the case of the superconducting phase, the higher order terms of the diagrammatic expansion are also essential here, and the zero-order calculations (which are equivalent to RMFT) do not lead to the stability of the nematic phase. In this sense, the presented analysis supports the hypothesis that the higher order effects resulting from electron correlations lead to the electron susceptibility of the wave function towards the C_4 symmetry breaking. Further analysis showed that that for a small distortion, there is a significant anisotropy between the directions (1.0) and $(0, 1)$ in the electron hopping expectation values (Fig .7 from [H4]), which corresponds to the situation known from the experiment [75, 76, 77]. However, this aspect requires more detailed analysis.

To summarize, we report the spontaneous C_4 symmetry breaking due to electron correlation, already at the level of the Hubbard model. Within such approach, the SC+N phase

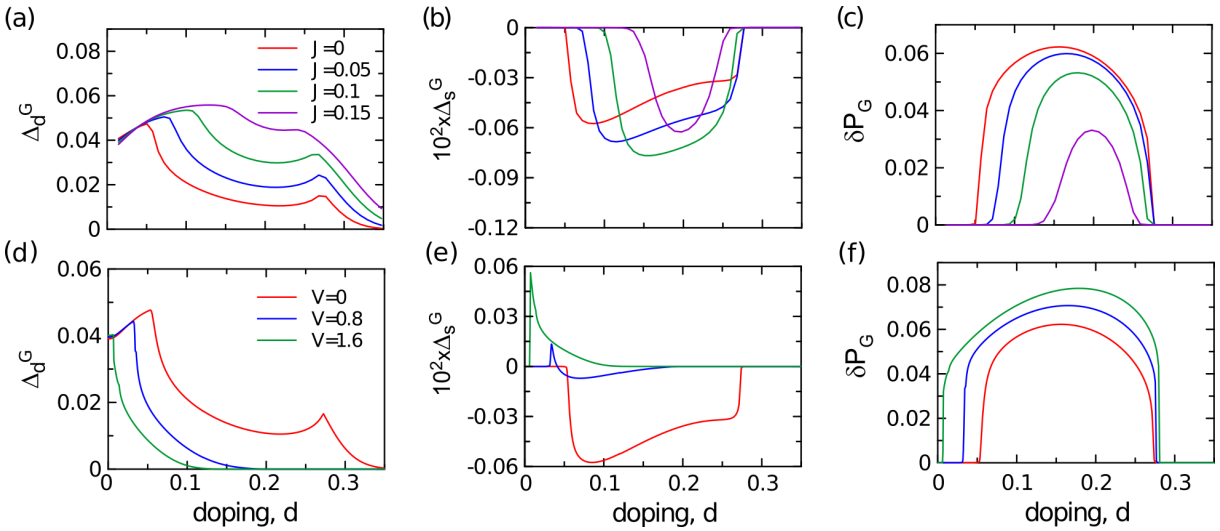

Figure 12: *d-wave* (a) and *s-wave* (b) superconducting gaps as well as the order parameter of the nematic phase (c) as a function of doping for the *t-J-U* model for selected values of the exchange integral J. Figures (d), (e), and (f) provide analogous results for the Hubbard model extended by the intersite Coulomb repulsion, for different values of V. For both models $U = 11.5$ was taken for the calculations. Figures taken from [H4].

stability region (coexistence of superconductivity and nematic phase) is quite robust, which would be destructive for the nodal direction appearance due to the *s-wave* component of the pairing in the SC+N state. However, for the *t-J-U* model, for which the agreement with principal features of the superconducting phase has been previously obtained (see Section 4.3), the nematicity is destroyed by the exchange interactions. As a result, the previously obtained properties can be preserved even after taking into account the nematic phase, which can still occur, but in a very limited area of doping, after considering the weak rhombohedral distortion and/or Coulomb intersite repulsion.

At the next stage the charge density wave (CDW) phase has been analyzed. The initial calculations were carried out within the SGA method, which is a modification of RMFT with statistical self-consistency conditions imposed [H5]. In general, the electron concentration modulation in the CDW phase (for the case of no magnetic ordering) is given by

$$n_i = n + \delta_n e^{i\mathbf{Q}\mathbf{R}_i}, \tag{7}$$

where n is the reference value, and δ_n is the modulation amplitude of the charge density wave that can be interpreted as a CDW order parameter. The simplest form of the CDW phase is defined by the modulation vector $\mathbf{Q} = (\pi, \pi)/a$. In such case, the system is divided into two sublattices. For one of them the concentration of electrons is smaller, and for the other correspondingly larger. According to the calculations carried out within the SGA method the considered CDW phase is not stable for the case of Hubbard and *t-J-U* models. Nevertheless, as shown in Fig. 13, after adding the intersite Coulomb repulsion term (*t-J-U-V* model), starting from a certain critical value of the V parameter, the charge ordering stability region appears and becomes wider as the V parameter is increased. It should be noted that the threshold value $V \approx 1.85$, above which the CDW phase appears in the phase diagram is so large that the superconductivity is already completely destroyed.

The results shown in the Fig. 13 cannot be directly related to the experimental picture, due to the fact that the theoretical approach leads to, the CDW phase appearance for too large dopings. Experimentally, it has been established that the CDW phase appears in the underdoped regime. In addition, the experimentally determined modulation vectors differ from those taken for the initial theoretical analysis. Namely, according to the available experimental data, charge modulation vectors are incommensurate and take the form $(0, Q)2\pi/a$ and $(Q, 0)2\pi/a$, where

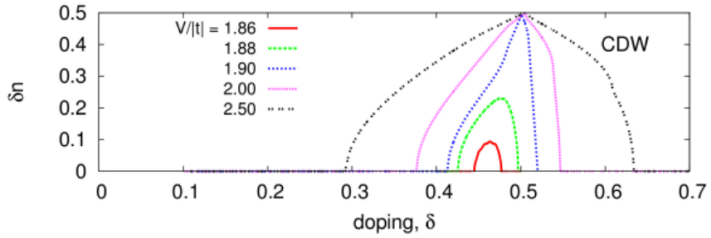

Figure 13: Modulation amplitude for the CDW phase for $\mathbf{Q} = (\pi, \pi)$ for the t-J-U-V model with $U = 20$, $J = 1/3$ and for selected values of V. Figures taken from [H5].

$Q \approx 0.25-0.3$ [80, 81, 82]. It is still unclear whether these two vectors are realized simultaneously in the cuprates, or two types of domains are formed within the sample in which only one of the measured vectors defines the form of CDW phase [83].

In order to examine the effect of the modulation vector on the theoretically determined CDW phase stability region, calculations have been carried out for the case of the $\mathbf{Q}$ vector which is close to the one that is actually measured experimentally, i.e. with $Q = 1/3$ [H5]. Moreover, the presence of the antiferromagnetic phase was taken into account in the calculations. The results for $\mathbf{Q} = (\pi, \pi)/a$ and $\mathbf{Q} = (1/3, 0)2\pi/a$ are shown in Figs. 14 (a) and (b), respectively. As can be seen, after changing the modulation vector, the CDW phase stability regime changes substantially and the order parameter maximum moves towards lower dopings, which brings theoretical results closer to the experimental data. In addition, antiferromagnetic phase (AF) appears close to the half-filling, which is also observed experimentally. Nevertheless, the calculated upper critical doping for the appearance of the AF ordering is too large in comparison with the experimental value [3]. As discussed in Appendix B to the paper [H5], the latter result can be significantly improved if an alternative scheme for determining the renormalization parameters in the AF phase is applied.

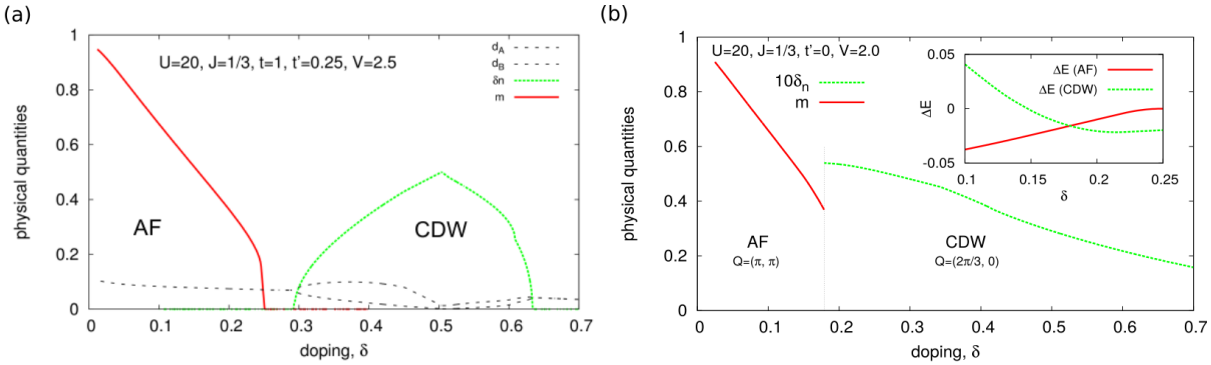

Figure 14: Phase diagram for the t-J-U-V model with the inclusion of the antiferromagnetic phase (with order parameter $m = n_\uparrow - n_\downarrow$) and the phase with the charge density wave [with order parameter δ_n defined in (7)] corresponding to the modulation vector $\mathbf{Q} = (\pi, \pi)/a$ (a) and $\mathbf{Q} = (1/3, 0)2\pi/a$ (b). Figures taken from [H5].

Due to the fact that the phase diagrams obtained as part of the preliminary calculations (within the SGA method) do not agree satisfactorily with the experimental picture [3, 7, 80], the calculations with the inclusion of the higher orders of our diagrammatic expansion were also carried out. This analysis was aimed at verifying whether this approach will allow to reconstruct the experimental situation, for which in the overdoped regime ($\delta_{\text{opt}} \approx 0.15-0.2$) the pure *d-wave* superconducting phase is stable, while for the underdoping the CDW phase appears. It should be noted, that the appearance of the Cooper pair density wave state (PDW) has been recently reported experimentally [6]. According to this study the modulation vector of the PDW phase is very similar to the one corresponding to the charge order modulation.

Therefore, we have analyzed the situation in which the superconducting phase adapts to the charge density wave by creating its own Cooper pair density modulation with the same vector **Q**. This leads to the PDW+CDW coexistence for which the modulation applies to electron concentration $n_{i\sigma} = \langle \hat{c}^{\dagger}_{i\sigma}\hat{c}_{i\sigma}\rangle_G$, electron hopping expectation values $P^G_{ij\sigma} = \langle \hat{c}^{\dagger}_{i\sigma}\hat{c}_{j\sigma}\rangle_G$, as well as anomalous averages which are responsible for the superconductivity $\Delta^G_{ij} = \langle \hat{c}^{\dagger}_{i\uparrow}\hat{c}^{\dagger}_{j\downarrow}\rangle_G$. The modulation amplitudes denoted by δn_{CDW}, $\delta P^{d,s',s'',x,x''}_{CDW}$, and $\delta\Delta^{d,s',x}_{PDW}$ correspond to the three aforementioned averages, respectively. The individual symbols in the superscripts d, s', s'', x', x'' correspond to the specific symmetries for the charge-density- and for the Cooper-pair-density-wave and are defined in detail in [H6]. In such case the modulation amplitudes play the role of order parameters for the complex PDW+CDW phase.

First, the calculations for the Hubbard model were carried out. The determined phase diagrams are shown in Fig. 15. As one can see the pure *d-wave* superconductivity (SC) begins to be stable below $\delta \approx 0.35$. Then the C_4 symmetry is spontaneously broken below $\delta \approx 0.28$ and the nematic phase coexisting with superconductivity (SC+N) is formed. In this phase there is a mixture of *d-wave* and *s-wave* symmetries and non-zero values of $P^G_{(1,0)} - P^G_{(0,1)}$ (see Fig. 11 and 12). Then, below $\delta \approx 0.2$ the CDW+PDW stabilty regime sets in. As can be seen in the Figure, non-zero values of all the modulation amplitudes considered here appear in this region. The nematic phase, which appears while reducing the doping, can be understood as a precursor phase of the CDW and PDW phases in which C_4 symmetry breaking takes place.

As you can see in the Fig. 13 the term $\sim V$ was necessary to stabilize the CDW phase within the SGA approximation (modification of the RMFT approach). However, by including the higher orders of the diagrammatic expansion within the DE-GWF method, one obtains the stability of the charge density modulated phase (this time co-existing with the PDW phase) already for the Hubbard model case for $V = 0$ (intrasite Coulomb interactions only). In addition, its stability area reaches up to $\delta \approx 0.2$, which better reflects the experimental situation. This is yet another example showing the limitations of the RMFT approximation and how significant are the higher order terms of the diagrammatic expansion for th description of the strongly correlated electron systems. A similar result for the Hubbard model, however, in the narrower range of dopings and without taking into account the nematic phase, was obtained as part of the Variational Cluster Approximation method (VCA) [31].

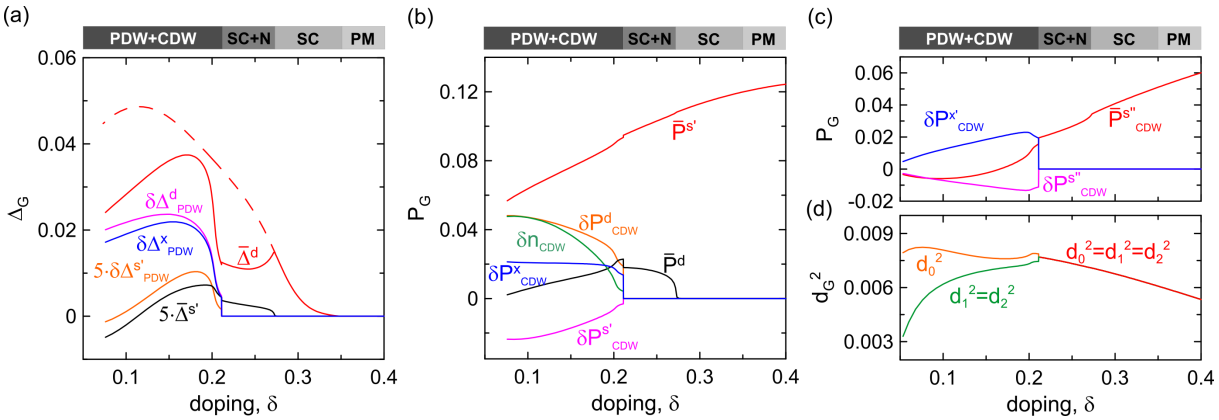

Figure 15: Phase diagram for the Hubbard model for $U = 18$. (a) The reference values of the *d-wave* ($\bar{\Delta}^d$) and extended *s-wave* ($\bar{\Delta}^{s'}$) SC gaps, as well as the modulation amplitudes $\delta\Delta^d_{PDW}$, $\delta\Delta^{x'}_{PDW}$ and $\delta\Delta^x_{PDW}$ as a function of doping; (b), (c) electron hopping expectation values corresponding to the *s-wave* ($\bar{P}^{s'}$, $\bar{P}^{s''}$) and *d-wave* ($\bar{P}^d$) symmetries, as well as the modulation amplitude δP^d_{CDW}, $\delta P^{s'}_{CDW}$, $\delta P^{s''}_{CDW}$, δP^x_{CDW}, and $\delta P^{x'}_{CDW}$ as a function of doping; (d) double occupancies on subsequent sublattice sites (0,1,2), which form a repeating pattern in the coexistent PDW+CDW phase. The doping stability ranges of subsequent phases is marked at the top of the Figures. Figure taken from [H6].

In spite of the interesting result obtained for the Hubbard model, it was still not possible to reconstruct the correct sequence of phases observed in this experiment [3, 7]. Therefore, at the next stage of the research, calculations were carried out for the *t-J-U* model, which had previously lead to a very good agreement with the experiments regarding the pure superconducting phase (see chapters 4.3, 4.4). As you can see in Fig. 16 after considering the term $\sim J$, the superconducting phase suppresses nematic ordering, resulting in a phase sequence similar to that known from experimental research. This means that in the overdoped regime we have a pure superconducting phase with *d-wave* gap symmetry, which creates the characteristic dome structure with the optimal doping $\delta_{\text{opt}} \approx 0.18$. Furthermore, in the underdoped regime $\delta < \delta_{\text{opt}}$ we observe the charge ordering [7, 80]. In our case, the CDW phase appears in coexistence with the PDW phase, which has also been verified in a compound from the cuprate family [6]. Modulation amplitudes which describe the CDW ordering increase as the doping decreases, which corresponds to the experimentally observed changes in the critical temperature for the formation of CDW phase with doping [84, 80]. Moreover, the obtained results show that the charge ordering competes with the *d-wave* superconducting phase. In the PDW+CDW stability region, the reference value responsible for the *d-wave* pairing is reduced relative to that corresponding to the situation when no modulated states are taken into account [cf. red dotted line in Fig. 16 (a)]. Similar competition between the two phases is also observed experimentally, where the critical temperature is reduced in the CDW stability regime [7, 84].

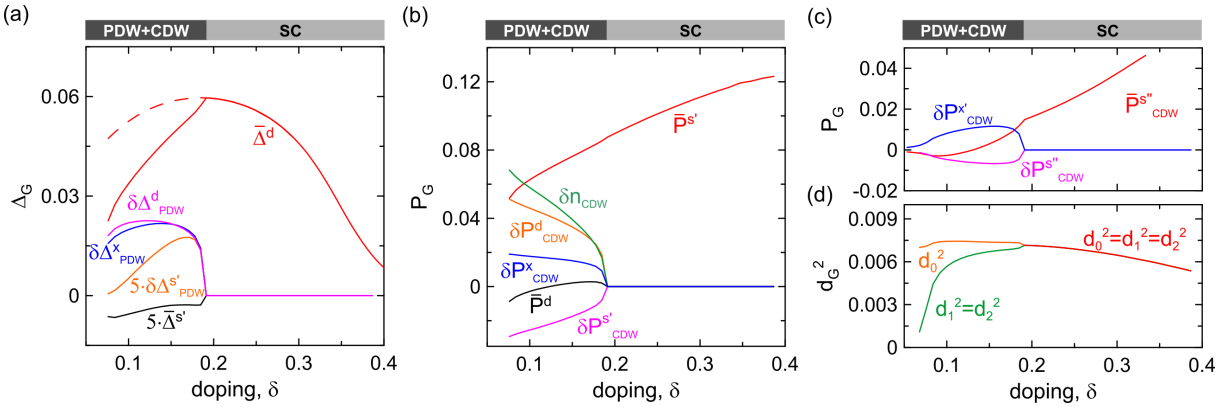

Figure 16: Phase diagram for the *t-J-U* model for $U = 18$. (a) The reference values of the *d-wave* ($\bar{\Delta}^d$) and extended *s-wave* ($\bar{\Delta}^{s'}$) SC gaps, as well as the amplitude modulations $\delta\Delta^d_{PDW}$, $\delta\Delta^{x'}_{PDW}$ and $\delta\Delta^x_{PDW}$ as a function of doping; (b), (c) electron hopping expectation values corresponding to the *s-wave* ($\bar{P}^{s'}$, $\bar{P}^{s''}$) and *d-wave* ($\bar{P}^d$) symmetries, as well as the modulation amplitudes δP^d_{CDW}, $\delta P^{s'}_{CDW}$, $\delta P^{s''}_{CDW}$, δP^x_{CDW}, and $\delta P^{x'}_{CDW}$ as a function of doping; (d) double occupancies on subsequent sublattice sites (0,1,2), which form a repeating pattern in the coexistent PDW+CDW phase. The doping stability ranges of subsequent phases is marked at the top of the Figures. Figure taken from [H6].

To summarize, when it comes to the charge ordered phase, the best agreement with the available experimental data was obtained for the *t-J-U* model with microscopic parameters close to those for which we have previously been able to reproduce quantitatively the principal properties of the pure superconducting phase of the cuprates. Formation of the CDW phase within our approach occurs due to the effects of electron correlation, which were accounted for by higher order terms of the diagrammatic expansion (DE-GWF method). Within such approach, it was possible to reconstruct the proper sequence of phases which is observed in the phase diagram for the cuprates with the *d-wave* superconducting phase in the overdoped regime and the charge ordering contained in the underdoped regime. In the latter the competition between the SC and CDW phases appear which also is reported experimentally. Nevertheless, according to available experimental data, in a large group of copper-based compounds, the dominant amplitude in terms of the CDW phase is that corresponding to the *d-wave* symmetry ($deltaP^d_{CDW}$). Within

our theoretical description $deltaP^{d}_{CDW}$ is higher as an absolute value than the other amplitudes, except for that corresponding to the modulation of the onsite electron concentration δn_{CDW} [see Fig. 16 (b) and (c)]. This inconsistency with the experimental picture requires further analysis, possibly going beyond the single-band models of the cuprates.

4.6 Superconductivity in the three-band model of cuprates (paper [H7])

Previous considerations regarding the copper-based compounds were carried out within an effective single-band approach. As mentioned in the Introduction, some experimental facts indicate the importance of explicit inclusion of the oxygen degrees of freedom in the description of the copper-based compounds [41, 42, 43, 40]. Therefore, calculations have been carried out for the case of the extended approach in which the oxygen orbitals of the Cu-O plane are included explicitly. For this purpose the so-called d-p model has been considered which consists of the $3d_{x^2-y^2}$ orbitals due to the copper atoms and $2p_x/2p_y$ orbitals due to the oxygen atoms. Typical hopping parameters were used for calculations: $t_{dp} = 1.13$ eV, $t_{pp} = 0.49$ eV, and the difference between d and p orbital atomic levels $\epsilon_{dp} = 3.57$ eV.

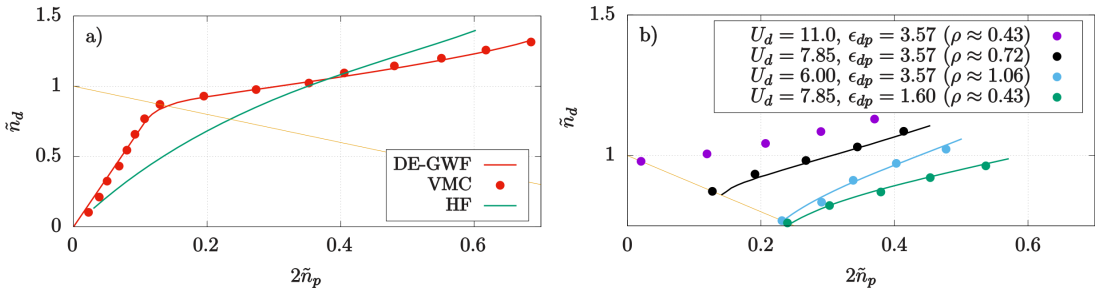

Figure 17: (a) The hole content distribution between the d and p orbitals ($\tilde{n}_d = 2 - n_d$, $\tilde{n}_p = 2 - n_p$) for the hole and electron doped case. The orange solid line corresponds to the parent compound and is defined by the equation $\delta = 1 - \tilde{n}_d - 2\tilde{n}_p = 0$. The upper right (bottom left) corner of the figure corresponds to hole (electron) doping. The calculations were carried out for $U_d = 7.85$ eV and $U_p = 4.1$ eV using the DE-GWF, VMC and HF methods; (b) The hole content distribution between the d and p orbitals for different values of the U_d and ϵ_{dp} parameters. For each case, the hole content distribution factor ($\rho = \Delta\tilde{n}_d/2\Delta\tilde{n}_p$) was determined by fitting the linear function to the calculated points. Figure taken from [H7].

As part of the initial analysis, calculations were carried out for the normal state with the use of the DE-GWF, variation Monte Carlo (VMC), as well as Hartee-Fock approximation (HF) methods. An extended version of the correlator was used for the VMC method, which explicitly takes into account the intersite correlations by using the so-called Jastrow coefficients (for more details see [H7]). Figure 17 shows the hole content distribution ($\tilde{n}_d = 2 - n_d$, $\tilde{n}_p = 2 - n_p$) between the copper and oxygen orbitals. As one can see, the results for the DE-GWF and VMC methods are practically the same, showing that the Gutzwiller wave function used within the DE-GWF approach takes into account the correlation effects with satisfactory accuracy and it is not necessary to include Jastrow correlators (VMC method). This result is also an additional test verifying the correctness of the implemented extension of the DE-GWF approach to the three-band model. The Hartee-Fock method, which neglects electron correlations leads to substantially different results and higher energy of the system than those derived from the DE-GWF and VMC methods (see Fig. 6 in [H7]). The available experimental data show that the hole content distribution factor ($\rho = \Delta\tilde{n}_d/2\Delta\tilde{n}_p$) for cuprates is $\rho \approx 0.2 - 1.0$, depending on the specific compound. For selected model parameters, the DE-GWF and VMC methods give the value $\rho = 0.72$, while HF leads to much larger unrealistic values of $\rho = 2.0$. This indicates that the low values of ρ measured for the cuprates are the result of strong correlations taken into account in the DE-GWF and VMC approaches.

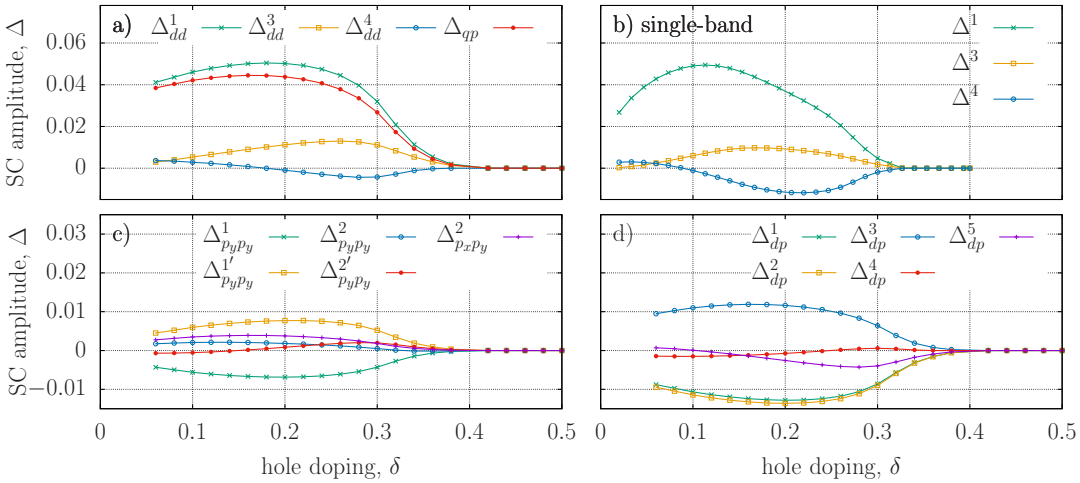

Figure 18: Pairing amplitudes between the orbitals taken into account in the three-band model: *d-d* (a), *p-p* (c), and *d-p* (d) as a function of doping for $U_p = 4.1$ eV and $U_d = 10.3$ eV. The superscripts appearing in the pairing amplitudes symbols, determine between which atomic sites the pairing takes place (for details see Fig. 3 in [H7]). Fig. (b) shows the pairing amplitudes for the first, third and fourth (the second is zero due to the *d-wave* pairing symmetry) nearest neighbor for a single-band Hubbard model with typical parameters ($t = -0.35$, $t' = 0.25|t|$,$U = 6$ eV). Figures taken from [H7].

According to recent experimental reports for the cuprates, the value of ρ is correlated with the maximum critical temperature [42]. Therefore, it is possible to make preliminary conclusions about the superconducting state already based on the results presented in the Fig. 17. As you can see in Fig. 17 (b) for smaller values of the Coulomb repulsion on the copper atoms we get higher values of the ρ parameter. Thus, smaller U_d should enhance superconductivity. This conclusion also agrees with the recent GW+DFT calculations [85], according to which the higher maximum critical temperature corresponds to the lower values of U_d ($HgBa_2CuO_4$-$T_C \approx 90K$, $U_d = 8.84$ eV and La_2CuO_4-$T_C \approx 40K$, $U_d = 9.61$ eV).

In the next stage of the research, calculations for the superconducting state were carried out within the DE-GWF method. Figure 18 shows correlated pairing amplitudes between different orbitals as a function of doping. The subsequent amplitudes are defined in Fig. 3 of the paper [H7]. As one can see, the dominant contribution to the superconducting phase results from the *d-d* paring between the copper nearest-neighbors (Δ^1_{dd}). This is also indicated by the fact that the amplitude Δ^1_{dd} essentially determines the behavior of the correlated quasi-particle gap (Δ_{qp}). The latter is the most representative pairing amplitude in the system due to the fact that it corresponds to the quasi-particle operators of creation and annihilation in states from the hybridized band. On the latter the gap opens in the superconducting state. As can be seen in the Figs. 18 (a) and (b), the doping dependences of the pairing amplitudes which correspond to subsequent copper nearest neighbors for the three-band model resemble the corresponding nearest neighbor pairings between the atomic sites for the case of the single band square-lattice model. Also, both approaches (single- and three-band) lead to a superconducting dome structure with a similar upper critical doping value for the appearance of the superconducting phase $\delta_c \approx 0.3 - 0.35$ and the optimal doping within $\delta_{\text{opt}} = 0.1 - 0.2$, which also agrees with the experimental data [2]. Moreover, the behavior of the calculated pairing amplitude in the (U_d, δ) plane [cf. Fig. 19 (a) and (b)] for the *d-p* model is similar to the one resulting from the single-band models [see Fig. 11 (d) and 3]. Namely, on the diagrams one can distinguish three regions: *(i)* weak correlations region where the pairing amplitude increases with increase of U_d (U for the single-band case); *(ii)* moderate correlations region placed around the maximum pairing amplitude as a function of U_d or U; *(iii)* strong correlations region, where the pairing amplitude

decreases with increasing U_d or U. The cuprates are placed in the strong correlations region, but near the moderate correlations regime. Therefore, the correlated superconducting gap (as well as the critical temperature) should be higher for compounds with a smaller value of U_d. It is because by reducing U_d we approach the moderate correlations region where the pairing amplitude is maximized. Such conclusion is in agreement with the the analysis of the ρ coefficient carried out earlier (Fig. 17).

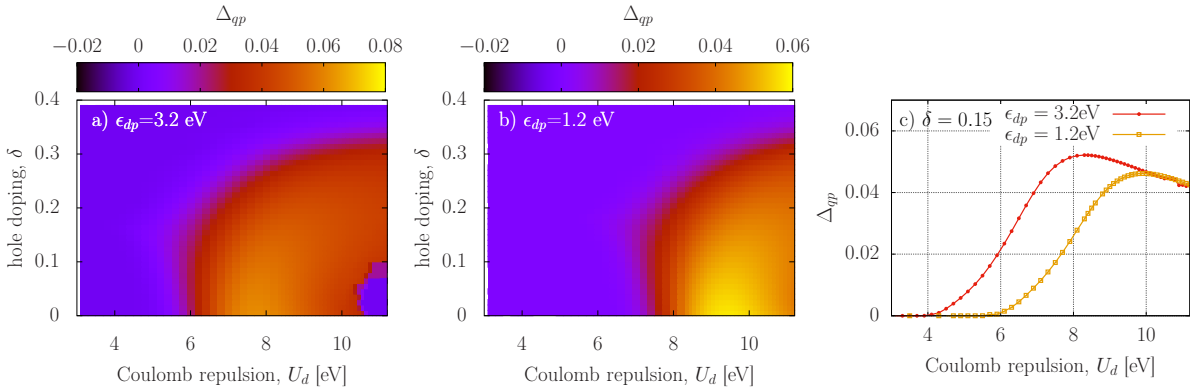

Figure 19: Quasiparticle superconducting gap as a function of doping (δ) and Coulomb repulsion at the d orbitals (U_d) for $\epsilon_{dp} = 3.2$ eV (a) and $\epsilon_{dp} = 1.3$ eV (b). Both cases correspond to $U_p = 4.1$ eV. Fig. (c) shows the Δ_{qp} as a function of U_d for the two selected values of ϵ_{dp}, for doping $\delta = 0.15$. Figure taken from [H7].

Despite the similarities between the two models, there are also differences. Namely, within the single-band approach, the energy associated with the lowest excited state equals to U and corresponds to an electron transfer between two singly occupied sites of the lattice, which leads to a double occupancy. On the other hand, for the three-band description, the lowest energy excitation corresponds to an electron transfer from a doubly occupied oxygen orbital to a singly occupied copper orbital. Such a process leads to an increase in the energy of the system by $\Delta E = U_d - U_p + \epsilon_{dp}$. In the d-p model, the value of ΔE determines the strength of the correlations. Thus, decreasing the value of ϵ_{dp} should move the entire SC phase stability region towards higher values of the U_d in the (U_d, δ) plane. This effect can be seen in the Fig. 19 where decreasing ϵ_{dp} by 2 eV leads to a shift of the SC stability regime towards higher U_d by the same value of ≈ 2 eV. Such behavior of the model leads to a situation in which lower values of both U_d and ϵ_{dp} correspond to compounds, which are closer to the moderate correlations regime, where the pairing amplitude is maximized. This in turn results in higher critical temperatures for those materials.

The spin-spin correlation functions between the d orbitals of the copper atoms were also determined for three selected modulation vectors. As can be seen in Fig. 20 the spin-spin correlation corresponding to the modulation vector $\mathbf{Q} = (\pi, \pi)$ is the dominant one and has a maximum for the undoped system. This corresponds to the experimental situation for the cuprates, where antiferromagnetic phase is observed for parent compounds and for very low values of hole doping ($\delta \lesssim 0.05$). Nevertheless, the correlation functions do not allow us to determine the value of the upper critical doping for the formation of antiferromagnetic order. Therefore, this aspect, as well as the question of the possible coexistence of the superconducting phase with antiferromagnetism for the low values of δ in the three-band model requires further research.

To summarize, in this Section we have shown that in general aspects, both single- and three-band approaches lead to similar results corresponding the the superconducting phase. This speaks for the correctness of the effective single-band description of the SC state in the cuprates. Nevertheless, explicit inclusion of the oxygen degrees of freedom seems necessary in order to carry out an accurate description of individual compounds from the cuprate family

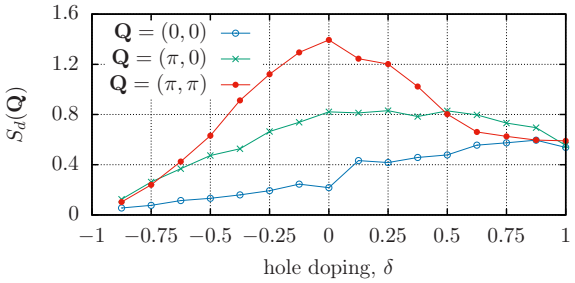

Figure 20: Spin-spin correlation functions between d orbitals vs. doping for three selected modulation vectors determined by the use of the VMC method. Figures taken from [H7].

and to map the differences between them. Such differences correspond for example to different values of the maximum critical temperature. The analysis of the hole distribution coefficient ρ presented here, which is related to this latter aspect, shows the qualitative agreement with the available experimental data [42]. In addition, the inclusion of oxygen degrees of freedom may play an important role in obtaining the full agreement for the case of the charge ordered phase [5] and the so-called pseudogap phase [7]. This, however, reaches beyond the scope of the analysis presented here.

4.7 Spontaneous FFLO superconducting phase in the model of iron-based compounds (papers [H8, H9])

In this Section we analyze the concept of a Fulde-Ferrell (FF) phase creation due to the mismatch of the Fermi-surface sheets in the model with interband pairing. As proposed by us in [H8], this type of phase may arise spontaneously in the absence of any external field, which in turn is necessary in the original concept by Fulde and Ferrell, as well as Larkin and Ovczinnikov [86, 87]. In such approach, the mismatch between the Fermi surface sheets can be compensated by the non-zero center-of-mass momentum of the Cooper pairs, which leads to the formation of the FF phase. The model selected for the analysis of the proposed effect, describes the two hole and two electron bands of an iron-based superconductors, which was supplemented with the singlet inter-band pairing term. The dispersion relations and the corresponding Fermi-surface sheets are shown in the Fig. 21, while the singlet pairing operators are defined by formula (4) in the [H8]. We consider a situation in which Cooper pairs can have a non-zero center-of-mass momentum ($\mathbf{Q}$), and the superconducting gap has the mixed *s-wave + extended s-wave* symmetry. As shown in [H8], in this model one can tune the mismatch between the two hole-like Fermi-surface sheets Δk_1 and two electron-like Fermi-surface sheets Δk_2 by changing the number of carriers in the system (see fig. 21). As a result, by setting the proper doping level, it is possible to create favorable conditions for the appearance of the proposed FF phase.

At first, a simplified model was analyzed, which consists of only two hole-like bands. In such situation, we have two concentric Fermi-surface sheets placed around the Γ point in the Brillouin zone, with pairing between them [see Fig. 21 (b)]. In Fig. 22 it is shown how the free energy of the system depends on the momentum of the Cooper pairs for two selected doping values. For $n = 1.75$, the superconducting state with $\mathbf{Q} = (0, 0)$ is going to be stable (a), while after increasing the doping of by 0.04, four minima in the free energy appear corresponding to the non-zero center-of-mass momentum of Cooper pairs (b). As one can see in Fig. 22 (d) the free energy for non-zero $\mathbf{Q}$ has a lower value than for $\mathbf{Q} = (0, 0)$. Thus, the state in which the superconducting current flows is going to be formed spontaneously. The fact that there are four equivalent minima located at the axes k_x and k_y results from the symmetry of the crystal lattice and from the symmetry of the superconducting gap (*s-wave*). Calculations were also carried out in a slightly different theoretical approach for *d-wave* symmetry of the gap. In such case, similar minima are located at the directions $k_x = k_y$ and $k_x = -k_y$ (see Fig. 6 in [H9]).

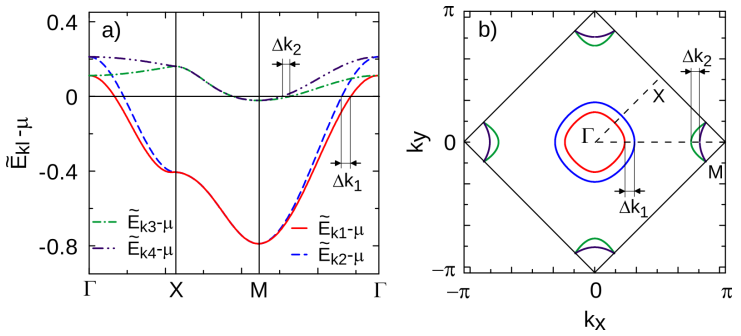

Figure 21: The electronic structure (a) and Fermi-surfaces sheets (b) for the considered four-band model with the band filling $n = 1.94$. The mismatch between the hole-like and the electron-like Fermi-surface sheets is described by the parameters Δk_1, Δk_2.

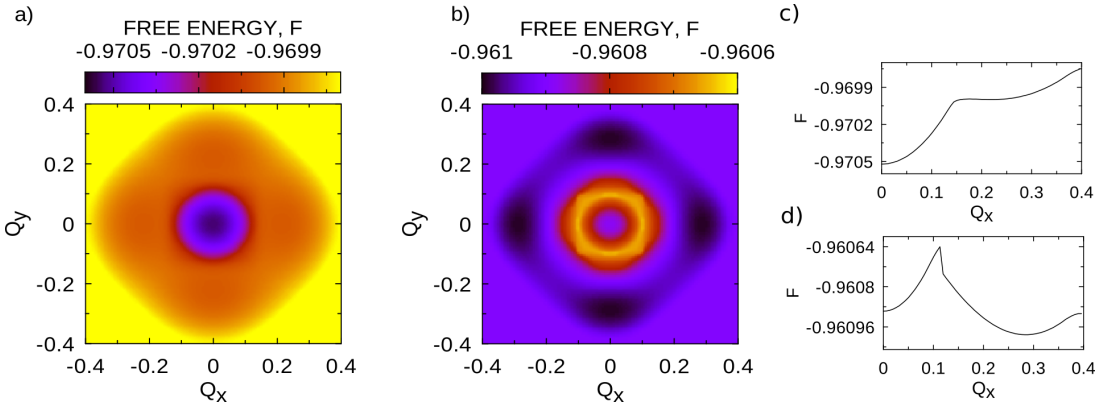

Figure 22: The free energy of the paired state as a function of the Cooper pairs center-of-mass momentum for $n = 1.75$ (a) and $n = 1.79$ (b) for a model describing the two hole-like bands of an iron-based superconductor. The pairing strengths have been set to $U_0 = 0.39$. Figures (c) and (d) show free energy for $n = 1.75$ and $n = 1.79$ respectively, as a function Q_x for $Q_y = 0$. Minima visible in (b) and (d) indicate the possibility of a spontaneous FF phase formation.

The phase diagram in the (T, n) plane [Fig. 23 (a)] resembles the one corresponding to the standard FFLO phase induced by the magnetic field [**Mask**, 88]. However, in the latter case, instead of the doping axis there is magnetic field induction axis. At the same time, in both cases the transition between the SC and FF phases is a discontinuous transition. This is indicated by a sudden drop in the pairing amplitudes corresponding to the *s-wave* and *extended s-wave* ($\Delta_{1Q}^{(0)}$ and $\Delta_{1Q}^{(1)}$) symmetries at the SC/FF border [cf. Fig. 23 (c) and (d)]. Also, the pairing amplitudes and $\mathbf{Q}$ vector absolute value have similar behavior as those presented in [89], which correspond to the conventional type of the FF phase. In the model under consideration, the situation corresponding to spin-singlet with orbital-triplet is equivalent to the spin-triplet with orbital-singlet case. Thus, the proposed FF phase can also appear with the spin-triplet pairing induced by the inter-orbital Hund's coupling. Such a scenario was considered in [H9]).

The proposed concept was also tested for the full four-band model. As one can see in Fig. 21, in such case the Fermi wave vector mismatch between the two hole-like Fermi surface sheets (marked by Δk_1) may be different from the one corresponding to the electron-like Fermi surface sheets (marked by Δk_2). Thus, in general we can consider a situation in which there are two different $\mathbf{Q}$ vectors, each of which leading to compensation of the mismatch in different pair of bands. Nevertheless, one should note the term, which corresponds to the Cooper pair transfer between the hole-like and electron-like bands. Assuming that there is no momentum change during transfer of Cooper pairs, it is necessary to minimize the energy of the system with respect to a single vector $\mathbf{Q}$, which corresponds to the whole system.

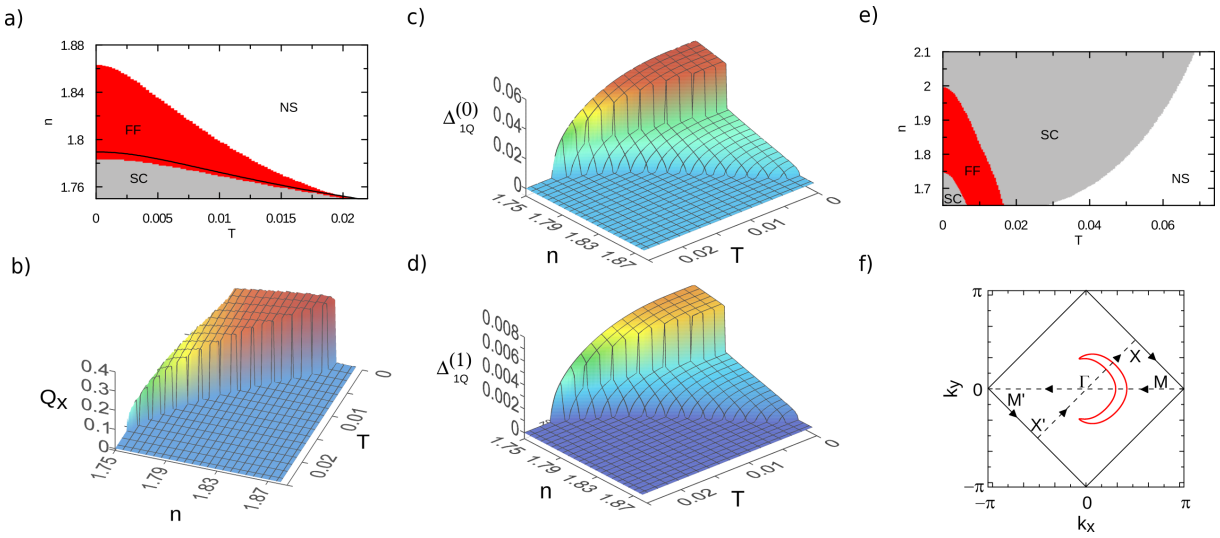

Figure 23: (a) Phase diagram at the (T, n) plane for the model describing two hole-like bands of an iron-based superconductor. The black continuous line marks the upper critical doping for the case when the FF phase is not taken into account in the calculations; (b) the Q_x component of the Cooper pairs center-of-mass momentum as a function of n and T, which correspond to the stability of the FF phase; (c) and (d) the *s-wave* and *extended s-wave* superconducting gap amplitudes as a function of n and T; (e) phase diagram at the (T, n) plane for $U_O = 0.39$ and $\gamma = 0.01$ for the four-band model; (f) the area occupied by unpaired particles originating from one of the hole-like bands for the band filling $n = 1.795$.

It has been shown that similarly as in the previous case also for the four-band model for certain doping values free energy minima appear, which correspond to non-zero $\mathbf{Q}$ vectors located on the axes k_x and k_y (see Fig. 8 in [H8]). The area of stability of the FF phase in the (T, n) phase diagram is shown in Fig. 23 (e). The phase transitions between the SC and FF phases are discontinuous similarly as in the two-band case. However, this time the phase diagram is quite unconventional. Namely, with increasing doping a transition between the FF and SC phase appear instead of the transition from the FF phase directly to the normal state as before [cf. fig. 23 (a)]. Nevertheless, the location of the FF phase stability region in the diagram is similar to that for the case of the simplified two-band model. This is due to the fact that the Cooper pair center-of-mass momentum vector $\mathbf{Q}$ is mainly determined by the shape of the two hole-like Fermi surface-sheets bands. This is because the superconducting gap for electron-like bands is significantly larger than for the hole-like. This means that despite non-zero values of Δk_2 for a given range of dopings, the pairing in the electron-like bands can exist without the necessity of compensating Δk_2 by the non-zero momentum of the Cooper pairs. Thus, the FF phase is induced due to the energetically beneficial Δk_1 compensation that occurs in the hole-like bands. This is also indicated by the shape of the depairing region in the Brillouin zone [Fig. **??** (f)], which is occupied by unpaired particles in one of the hole-like bands. All particles in the electron bands are paired; therefore, the deparing region is located near the underlying Fermi surface corresponding to one of the hole-like bands.

To summarize, the proposed unconventional Fulde-Ferrell phase can be stable in materials in which superconductivity has a multiband character with dominant interband pairing and appropriate Fermi surface topology. A group of materials that could meet these conditions are iron-based high temperature superconductors. As shown, for the two- and four-band model appropriate for this family of materials, the FF phase can be induced within a particular doping range. The basic characteristics of the proposed FF phase are similar to those observed in the standard situation where the non-zero momentum of Cooper pairs is induced by the presence of an external magnetic field. The presented concept is also interesting due to the possibility of obtaining a material in which the superconducting current is induced, in the absence of any

external magnetic or electric field. Nevertheless, the question whether the dominant interband pairing channel can appear in the iron-pnictides or other compounds still remains open. It should also be noted that until now the proposed effect has not been observed experimentally. Therefore, this concept requires further analysis, both theoretical and experimental.

4.8 Summary

We have carried our a detailed analysis of the effective single-band models to the description of the copper-ased superconductors. According to our research, the important elements of the theoretical approach, that allow to obtain the proper agreement with the principal experimental observations, are: *(i)* the incorporation of the exchange interaction term ($\sim J$), which in an effective manner represents the *dd* superexchange via the antibonding $2p_\sigma$ states due to oxygen; *(ii)* small but non-zero number of double occupancies which is determined by the value of the onsite Coulomb repulsion; *(iii)* strong electron correlations effects taken into account at level higher than RMFT. All those features appear in the theoretical description based on the *t*-*J*-*U* model with the application of the DE-GWF method in the higher orders of the expansion. With the use of such a description of the copper-oxide plane, the following results were obtained:

- Good agreement with the available experimental data was obtained for the case of principal features of the superconducting state in the cuprates. Namely, *(i)* the calculated correlated pairing amplitude reflects the characteristic dome structure as a function of doping for $\lesssim 0.35 - 0.4$ with the optimal doping $\sim 0.1 - 0.2$; *(ii)* the theoretical results show the asymmetry between the electron and hole doped sites of the phase diagram in favor of the latter in qualitative agreement with experiment; *(iii)* the transition between the non-BCS and BCS-like paired states appears close to the optimal doping with the non-BCS regime contained within the underdoped regime [quantitative agreement with experiment for $\Delta E_{\mathrm{kin}}(\delta)$]; *(iv)* calculated Fermi velocity in the nodal direction, Fermi momentum and the effective mass are weakly dependent on doping and they agree quantitatively with the available experimental data.

- The physical picture of the superconducting state based on the *t*-*J*-*U* model is preserved after extending the model with the two-site interaction terms (correlation hopping and intersite Coulomb repulsion). Such situation indicates the universality of the approach, i.e. the correct choice of the minimal model for a realistic description of selected properties of copper-based high-temperature superconductors.

- The analysis of the copper-oxide bilayer structure indicates that the principal properties of the superconducting state oobtained within the single-band *t*-*J*-*U* model do not change essentially as a result of inter-layer effects. However, in systems with more than one Cu-O layers in the unit cell, the increase of the maximum critical temperature is mainly caused by the interplanar pair hopping processes. Additionally, for the bilayer model, a relatively good agreement has been achieved between the theoretical and experimental results for the Bi-2212 compound.

- The proper sequence of phases on the phase diagram has been reproduced, with the pure *d-wave* superconducting phase above the optimal doping and the charge ordered phase in the underdoped regime, where a competition between the SC and CDW phases appear. Additionally, the phase with charge modulation appears in the form coexisting with the Cooper pair density wave (PDW + CDW). The latter was observed experimentally in recent years. The aspect of the proper balance between the amplitudes of modulation that correspond to particular symmetries still need further research.

Within the presented research, the DE-GWF approach was also extended to the case of the three-band model of the cuprates, which explicitly includes oxygen degrees of freedom. In some

general aspects, one- and three-band approaches lead to similar results for the superconducting phase, which supports the correctness of the effective single-band description and the results described above. Nevertheless, explicit includion of oxygen degrees of freedom seems necessary in order to carry out a detailed description of individual compounds from the cuprate family and to reconstruct the differences that exist between them, such as different values of the maximum critical temperature. The analysis of the hole content distrubution factor ρ, which is related to this last aspect, shows qualitative agreement with the available experimental data.

The presented theoretical studies on copper-based superconductors based on the paradigm of strong correlations led to results that uniformly reconstruct the fundamental properties of a part of the cuprate phase diagram. Nevertheless, it has still not been possible to create a complete theory which would describe all of the unconventional phases observed in this family of compounds. In particular, the proper description of the pseudogap phase and its relationship with other phases as superconductivity or e.g. CDW or PDW phases, is still lacking. It seems that for this purpose it may be necessary to conduct a similar analysis, which, however, takes into account both the effects resulting from strong local correlations (as here), as well as long-range quantum fluctuations. This approach is characterized by a much higher degree of complexity and requires further detailed analysis.

As part of the study of unconventional superconductivity, an Fulde-Ferrell type of phase was also proposed, which may appear spontaneously, i.e. without applying any external factor in the form of a magnetic or electric field. According to the analyzed concept, in materials with predominant inter-band pairing, the mismatch between two Fermi-surfaces sheets can be compensated by the non-zero center-of-mass momentum of the Cooper pairs which leads to the formation of the FF phase. This idea was tested within a model appropriate for the description of iron-based superconductors. As shown, the formation of the FF phase can be induced by setting the proper doping level of the system. The idea is also interesting due to the possibility of obtaining a material in which the superconducting current is induced without any external field. Nevertheless, it remains debatable whether a dominant inter-band pairing channel may appear in the iron-pnictides. This last aspect requires further analysis.

4.9 References

[1] M. Ogata, H. Fukuyama. "The t – J model for the oxide high- T c superconductors". *Rep. Prog. Phys.* **71** (2008), 036501.

[2] Patrick A. Lee, Naoto Nagaosa, Xiao-Gang Wen. "Doping a Mott insulator: Physics of high-temperature superconductivity". *Rev. Mod. Phys.* **78** (2006), 17.

[3] B. Keimer, S. A. Kivelson, M. R. Norman, S. Uchida, J. Zaanen. "From quantum matter to high-temperature superconductivity in copper oxides". *Nature* **518** (2015), 179.

[4] M. Hashimoto, M. Vishik, R.-H. He, T. P. Devereaux, Z.-X. Shen. "Energy gaps in high-transition-temperature cuprate superconductors". *Nature Physics* **10** (2014), 483.

[5] R Comin, R. Sutarto, F. He, E. H. da Silva Neto, L. Chauviere, A. Fraño, R. Liang, W. N. Hardy, D. A. Bonn, Y. Yoshida, H. Eisaki, A. J. Achkar, D. G Hawthorn, B. Keimer, G. A. Sawatzky, A. Damascelli. "Symmetry of charge order in cuprates". *Nature Materials* **14** (2015), 796.

[6] M. H. Hamidian, S. D. Edkins, S. H. Joo, A. Kostin, H. Eisaki, S. Uchida, M. J. Lawler, E.-A. Kim, A. P. Mackenzie, K. Fujita, J. Lee, J. C Séamus Davis. "Detection of a Cooper-pair density wave in Bi2Sr2CaCu2O8+x". *Nature* **532** (2016), 343.

[7] S. Badoux, W. Tabis, F. Laliberté, G. Grissonnanche, B. Vignolle, D. Vignolles, J. Béard, D. A. Bonn, W. N. Hardy, R. Liang, N. Doiron-Leyraud, L. Taillefer, C. Proust. "Change of carrier density at the pseudogap critical point of a cuprate superconductor". *Nature* **531** (2016), 210.

[8] P. W. Anderson. *in Frontiers and Borderlines in Many Particle Physics, edited by R. A. Broglia and J. R. Schrieffer, pp. 1-47* (North-Holland, Amsterdam, 1988).

[9] P. W. Andrerson. "More is Different". *Science* **177** (1972), 393.

[10] V. N. Krasnov, S.-O. Katterwe, A. Rydh. "Signatures of the electronic nature of pairing in high-Tc superconductors obtained by non-equilibrium boson spectroscopy". *Nat. Commun.* **4** (2013), 2970.

[11] D. J. Scalapino. "A common thread: The pairing interaction for unconventional superconductors". *Rev. Mod. Phys.* **84** (2012), 1383.

[12] R. Szczśniak, A. P. Durajski. "The Energy Gap in the (Hg1xSnx)Ba2Ca2Cu3O8+ySuperconductor". *Journal of Superconductivity and Novel Magnetism* **27** (2014), 1363–1367.

[13] R. Szczśniak, A. P. Durajski. "Description of High-Temperature Superconducting State in BSLCO Compound". *Journal of Superconductivity and Novel Magnetism* **28** (2015), 19–24.

[14] S. Johnston, F. Vernay, B. Moritz, Z.-X. Shen, N. Nagaosa, J. Zaanen, T. P. Devereaux. "Systematic study of electron-phonon coupling to oxygen modes across the cuprates". *Phys. Rev. B* **82** (2010), 064513.

[15] F. C. Zhang, T. M. Rice. "Effective Hamiltonian for the superconducting Cu oxides". *Phys. Rev. B* **37** (1988), 3759.

[16] K. A. Chao, J Spałek, A. M. Oleś. "Kinetic exchange interaction in a narrow s-band". *J. Phys. C* **10** (1977), L271.

[17] K. B. Lyons, P. A. Fleury, L. F. Schneemeyer, J. V. Waszczak. "Spin fluctuations and superconductivity in $Ba_2YCu_3O_{6+\delta}$". *Phys. Rev. Lett.* **60** (1988), 732–735.

[18] Shunji Sugai, Shin-ichi Shamoto, Masatoshi Sato. "Two-magnon Raman scattering in $(La_{1-x}Sr_x)_2CuO_4$". *Phys. Rev. B* **38** (1988), 6436–6439.

[19] G. Blumberg, P. Abbamonte, M. V. Klein, W. C. Lee, D. M. Ginsberg, L. L. Miller, A. Zibold. "Resonant two-magnon Raman scattering in cuprate antiferromagnetic insulators". *Phys. Rev. B* **53** (1996), R11930–R11933.

[20] P. Bourges, H. Casalta, A. S. Ivanov, D. Petitgrand. "Superexchange Coupling and Spin Susceptibility Spectral Weight in Undoped Monolayer Cuprates". *Phys. Rev. Lett.* **79** (1997), 4906–4909.

[21] B. Edegger, V. N. Muthukumar, C. Gros. "Gutzwiller–RVB theory of high-temperature superconductivity: Results from renormalized mean-field theory and variational Monte Carlo calculations". *Advances in Physics* **56** (2007), 927–1033.

[22] F. C. Zhang, C. Gros, T. M. Rice, H. Shiba. "A renormalised Hamiltonian approach to a resonant valence bond wavefunction". *Superconductor Science and Technology* **1** (1988), 36.

[23] E. Dagotto. "Correlated electrons in high-temperature superconductors". *Rev. Mod. Phys.* **66** (1994), 763–840.

[24] Arun Paramekanti, Mohit Randeria, Nandini Trivedi. "Projected Wave Functions and High Temperature Superconductivity". *Phys. Rev. Lett.* **87** (2001), 217002.

[25] Leonardo Spanu, Massimo Lugas, Federico Becca, Sandro Sorella. "Magnetism and superconductivity in the $t-t^{'}-J$ model". *Phys. Rev. B* **77** (2008), 024510.

[26] Sandeep Pathak, Vijay B. Shenoy, Mohit Randeria, Nandini Trivedi. "Competition between Antiferromagnetic and Superconducting States, Electron-Hole Doping Asymmetry, and Fermi-Surface Topology in High Temperature Superconductors". *Phys. Rev. Lett.* **102** (2009), 027002.

[27] Philippe Corboz, T. M. Rice, Matthias Troyer. "Competing States in the t-J Model: Uniform d-Wave State versus Stripe State". *Phys. Rev. Lett.* **113** (2014), 046402.

[28] Steven R. White, D. J. Scalapino. "Competition between stripes and pairing in a $t - t^{'} - J$ model". *Phys. Rev. B* **60** (1999), R753–R756.

[29] A. Himeda, T. Kato, M. Ogata. "Stripe States with Spatially Oscillating d-Wave Superconductivity in the Two-Dimensional $t - t^{'} - J$ Model". *Phys. Rev. Lett.* **88** (2002), 117001.

[30] Yuxuan Wang, Daniel F. Agterberg, Andrey Chubukov. "Coexistence of Charge-Density-Wave and Pair-Density-Wave Orders in Underdoped Cuprates". *Phys. Rev. Lett.* **114** (2015), 197001.

[31] J. P. L. Faye, D. Sénéchal. "Interplay between d-wave superconductivity and a bond-density wave in the one-band Hubbard model". *Phys. Rev. B* **95** (2017), 115127.

[32] Hermann Freire, Vanuildo S. de Carvalho, Catherine Pépin. "Renormalization group analysis of the pair-density-wave and charge order within the fermionic hot-spot model for cuprate superconductors". *Phys. Rev. B* **92** (2015), 045132.

[33] Krzysztof Byczuk, Jozef Spałek. "Transition temperature and a spatial dependence of the superconducting gap for multilayer high-temperature superconductors". *Phys. Rev. B* **53** (1996), R518–R521.

[34] R. Rüger, L. F. Tocchio, R. Valentí, C. Gros. "The phase diagram of the square lattice bilayer Hubbard model: a variational Monte Carlo study". *New Journal of Physics* **16** (2014), 033010.

[35] Voo K.-K. "Ground states of bilayered and extended t-J-U models". *Physics Letters A* **379** (2015), 1743.

[36] K. Nishiguchi, K. Kuroki, R. Arita, T. Oka, H. Aoki. "Superconductivity assisted by interlayer pair hopping in multilayered cuprates". *Phys. Rev. B* **88** (2013), 014509.

[37] T. A. Maier, D. J. Scalapino. "Pair structure and the pairing interaction in a bilayer Hubbard model for unconventional superconductivity". *Phys. Rev. B* **84** (2011), 180513.

[38] P. Plakida. *High-Temperature Cuprate Superconductors, Chapters 5, 7* ((Springer, 2010)).

[39] Andrea Damascelli, Zahid Hussain, Zhi-Xun Shen. "Angle-resolved photoemission studies of the cuprate superconductors". *Rev. Mod. Phys.* **75** (2003), 473–541.

[40] Y. Sakurai, M. Itou, B. Barbiellini, P. E. Mijnarends, R. S. Markiewicz, S. Kaprzyk, J.-M. Gillet, S. Wakimoto, M. Fujita, S. Basak, Yung Jui Wang, W. Al-Sawai, H. Lin, A. Bansil, K. Yamada. "Imaging Doped Holes in a Cuprate Superconductor with High-Resolution Compton Scattering". *Science* **332**.6030 (2011), 698–702.

[41] Guo-qing Zheng, Yoshio Kitaoka, Kenji Ishida, Kunisuke Asayama. "Local Hole Distribution in the CuO2 Plane of High-Tc Cu-Oxides Studied by Cu and Oxygen NQR/NMR". *Journal of the Physical Society of Japan* **64** (1995), 2524–2532.

[42] D. Rybicki, M. Jurkutat, S. Reichardt, C. Kapusta, J. Haase. "Perspective on the phase diagram of cuprate high-temperature superconductors". *Nat. Commun.* **7** (2016), 11413.

[43] W. Ruan, C. Hu, J. Zhao, P. Cai, Y. Peng, C. Ye, R. Yu, X. Li, Z. Hao, C. Jin, X. Zhou, Z.-Y. Weng, Y. Wang. "Relationship between the parent charge transfer gap and maximum transition temperature in cuprates". *Science Bulletin* **61** (2016), 1826.

[44] Cédric Weber, Kristjan Haule, Gabriel Kotliar. "Optical weights and waterfalls in doped charge-transfer insulators: A local density approximation and dynamical mean-field theory study of $La_{2-x}Sr_xCuO_4$". *Phys. Rev. B* **78** (2008), 134519.

[45] Ara Go, Andrew J. Millis. "Spatial Correlations and the Insulating Phase of the High-T_c Cuprates: Insights from a Configuration-Interaction-Based Solver for Dynamical Mean Field Theory". *Phys. Rev. Lett.* **114** (2015), 016402.

[46] Y. F. Kung, C.-C. Chen, Yao Wang, E. W. Huang, E. A. Nowadnick, B. Moritz, R. T. Scalettar, S. Johnston, T. P. Devereaux. "Characterizing the three-orbital Hubbard model with determinant quantum Monte Carlo". *Phys. Rev. B* **93** (2016), 155166.

[47] C. Weber, C. Yee, K. Haule, G. Kotliar. "Scaling of the transition temperature of hole-doped cuprate superconductors with the charge-transfer energy". *EPL (Europhysics Letters)* **100** (2012), 37001.

[48] T. Yanagisawa, M. Miyazaki, K. Yamaji. "Incommensurate Antiferromagnetism Coexisting with Superconductivity in Two-Dimensional d-p Model". *J. Phys. Soc. Jpn.* **78** (2009), 013706.

[49] A. Avella, F. Mancini, F. Paolo Mancini, E. Plekhanov. "Emery vs. Hubbard model for cuprate superconductors: a composite operator method study". *The European Physical Journal B* **86** (2013), 265.

[50] H Ebrahimnejad, G. A Sawatzky, M. Berciu. "The dynamics of a doped hole in a cuprate is not controlled by spin fluctuations". *Nature Physics* **10** (2014), 951.

[51] H. Ebrahimnejad, G. A. Sawatzky, M. Berciu. "Differences between the insulating limit quasiparticles of one-band and three-band cuprate models". *Journal of Physics: Condensed Matter* **28** (2016), 105603.

[52] H. Hosono, K. Kuroki. "Iron-based superconductors: Current status of materials and pairing mechanism". *Physica C* **514** (2015), 399.

[53] Jozef Spałek. "t-J model then and now: a personal perspective from pioneering times". *Acta Phys. Polon. A* **111** (2012), 409.

[54] Guy Deutscher, Andrés Felipe Santander-Syro, Nicole Bontemps. "Kinetic energy change with doping upon superfluid condensation in high-temperature superconductors". *Phys. Rev. B* **72** (2005), 092504.

[55] F. Carbone, A. B. Kuzmenko, H. J. A. Molegraaf, E. van Heumen, V. Lukovac, F. Marsiglio, D. van der Marel, K. Haule, G. Kotliar, H. Berger, S. Courjault, P. H. Kes, M. Li. "Doping dependence of the redistribution of optical spectral weight in $Bi_2Sr_2CaCu_2O_{8+\delta}$". *Phys. Rev. B* **74** (2006), 064510.

[56] C. Giannetti, F. Cilento, S. Dal Conte, G. Coslovich, F. Ferrini, H. Molegraaf, M. Raichle, R. Liang, H. Eisaki, M. Greven, A. Damascelli, D. van der Marel, F. Parmigiani. "Revealing the high-energy electronic excitations underlying the onset of high-temperature superconductivity in cuprates". *Nat. Commun.* **2** (2011), 1.

[57] D. van der Marel, J. van Elp, G. A. Sawatzky, D. Heitmann. "X-ray photoemission, bremsstrahlung isochromat, Auger-electron, and optical spectroscopy studies of Y-Ba-Cu-O thin films". *Phys. Rev. B* **37** (1988), 5136–5141.

[58] A. Fujimori. "Character of doped oxygen holes in high-T_c Cu oxides". *Phys. Rev. B* **39** (1989), 793–796.

[59] H. Eskes, L. H. Tjeng, G. A. Sawatzky. "Cluster-model calculation of the electronic structure of CuO: A model material for the high-T_c superconductors". *Phys. Rev. B* **41** (1990), 288–299.

[60] A. A. Kordyuk, S. V. Borisenko, A. N. Yaresko, S.-L. Drechsler, H. Rosner, T. K. Kim, A. Koitzsch, K. A. Nenkov, M. Knupfer, J. Fink, R. Follath, H. Berger, B. Keimer, S. Ono, Yoichi Ando. "Evidence for CuO conducting band splitting in the nodal direction of $Bi_2Sr_2CaCu_2O_{8+\delta}$". *Phys. Rev. B* **70** (2004), 214525.

[61] S. V. Borisenko, A. A. Kordyuk, V. Zabolotnyy, J. Geck, D. Inosov, A. Koitzsch, J. Fink, M. Knupfer, B. Büchner, V. Hinkov, C. T. Lin, B. Keimer, T. Wolf, S. G. Chiuzb ăian, L. Patthey, R. Follath. "Kinks, Nodal Bilayer Splitting, and Interband Scattering in $YBa_2Cu_3O_{6+x}$". *Phys. Rev. Lett.* **96** (2006), 117004.

[62] X. J. Zhou, T. Yoshida, A. Lanzara, P. V. Bogdanov, S. A. Kellar, K. M. Shen, W. L. Yang, F. Ronning, T. Sasagawa, T. Kakeshita, T. Noda, H. Eisaki, S. Uchida, C. T. Lin, F. Zhou, J. W. Xiong, W. X. Ti, Z. X. Zhao, A. Fujimori, Z. Hussain, Z.-X. Shen. "Universal nodal Fermi velocity". **423** (2003), 398.

[63] W. J. Padilla, Y. S. Lee, M. Dumm, G. Blumberg, S. Ono, Kouji Segawa, Seiki Komiya, Yoichi Ando, D. N. Basov. "Constant effective mass across the phase diagram of high-T_c cuprates". *Phys. Rev. B* **72** (2005), 060511.

[64] J. E. Hirsch, F. Marsiglio. "Superconducting state in an oxygen hole metal". *Phys. Rev. B* **39** (1989), 11515–11525.

[65] F. Marsiglio, J. E. Hirsch. "Hole superconductivity and the high-T_c oxides". *Phys. Rev. B* **41** (1990), 6435–6456.

[66] N. P. Armitage, D. H. Lu, C. Kim, A. Damascelli, K. M. Shen, F. Ronning, D. L. Feng, P. Bogdanov, X. J. Zhou, W. L. Yang, Z. Hussain, P. K. Mang, N. Kaneko, M. Greven, Y. Onose, Y. Taguchi, Y. Tokura, Z.-X. Shen. "Angle-resolved photoemission spectral function analysis of the electron-doped cuprate $Nd_{1.85}Ce_{0.15}CuO_4$". *Phys. Rev. B* **68** (2003), 064517.

[67] Seung Ryong Park, D. J. Song, C. S. Leem, Chul Kim, C. Kim, B. J. Kim, H. Eisaki. "Angle-Resolved Photoemission Spectroscopy of Electron-Doped Cuprate Superconductors: Isotropic Electron-Phonon Coupling". *Phys. Rev. Lett.* **101** (2008), 117006.

[68] I. M. Vishik, W. S. Lee, F. Schmitt, B. Moritz, T. Sasagawa, S. Uchida, K. Fujita, S. Ishida, C. Zhang, T. P. Devereaux, Z. X. Shen. "Doping-Dependent Nodal Fermi Velocity of the High-Temperature Superconductor $Bi_2Sr_2CaCu_2\mathbf{O}_{8+\delta}$ Revealed Using High-Resolution Angle-Resolved Photoemission Spectroscopy". *Phys. Rev. Lett.* **104** (2010), 207002.

[69] Gil Drachuck, Elia Razzoli, Rinat Ofer, Galina Bazalitsky, R. S. Dhaka, Amit Kanigel, Ming Shi, Amit Keren. "Linking dynamic and thermodynamic properties of cuprates: An angle-resolved photoemission study of $(Ca_xLa_{1-x})(Ba_{1.75-x}La_{0.25+x})Cu_3O_y$ ($x = 0.1$ and 0.4)". *Phys. Rev. B* **89** (2014), 121119.

[70] T. A. Zaleski, T. K. Kopeć. "Dependence of the superconducting critical temperature on the number of layers in a homologous series of high-T_c cuprates". *Phys. Rev. B* **71** (2005), 014519.

[71] O. K. Andersen, A. I. Liechtenstein, O. Jepsen, F. Paulsen. "LDA energy bands, low-energy hamiltonians,t', t", $t_\perp$(k) and $J_\perp$". *J. Phys. Chem. Sol.* **56** (1995), 1573.

[72] Guo-meng Zhao. "Precise determination of the superconducting gap along the diagonal direction of $Bi_2Sr_2CaCu_2O_{8+y}$: Evidence for an extended *s*-wave gap symmetry". *Phys. Rev. B* **75** (2007), 140510.

[73] H. Ding, J. C. Campuzano, A. F. Bellman, T. Yokoya, M. R. Norman, M. Randeria, T. Takahashi, H. Katayama-Yoshida, T. Mochiku, K. Kadowaki, G. Jennings. "Momentum Dependence of the Superconducting Gap in $Bi_2Sr_2CaCu_2O_8$". *Phys. Rev. Lett.* **74** (1995), 2784–2787.

[74] D. Fournier, G. Levy, Y. Pennec, J. L. McChesney, A. Bostwick, E. Rotenberg, R. Liang, W. N. Hardy, D. A. Bonn, I. S. Elfimov, A. Damascelli. "Loss of nodal quasiparticle integrity in underdoped YBa2Cu3O6+x". *Nature* **6** (2010), 905.

[75] M. J. Lawler, K. Fujita, J. Lee, A. R. Schmidt, Y. Kohsaka, C. K. Kim, H. Eisaki, S. Uchida, J. C. Davis, J. P. Sethna, E. -A. Kim. "Intra-unit-cell electronic nematicity of the high-Tc copper-oxide pseudogap states". *Nature* **466** (2010), 347.

[76] R. Daou, J. Chang, D. LeBoeuf, O. Cyr-Choinière, F. Laliberté, N. Doiron-Leyraud, B. J. Ramshaw, R. Liang, D. A. Bonn, W. N. Hardy, L. Taillefer. "Broken rotational symmetry in the pseudogap phase of a high-Tc superconductor". *Nature* **463** (2010), 519.

[77] V. Hinkov, D. Haug, B. Fauqué, P. Bourges, Y. Sidis, A. Ivanov, C. Bernhard, C. T. Lin, B. Keimer. "Electronic Liquid Crystal State in the High-Temperature Superconductor YBa2Cu3O6.45". *Science* **319** (2008), 597–600.

[78] D. Pelc, M. Vučković, H. -J. Grafe, S. -H. Baek, M. Požek. "Unconventional charge order in a co-doped high-Tc superconductor". *Nat. Commun* **7** (2016), 12775.

[79] A. J. Achkar, M. Zwiebler, Christopher McMahon, F. He, R. Sutarto, Isaiah Djianto, Zhihao Hao, Michel J. P. Gingras, M. Hücker, G. D. Gu, A. Revcolevschi, H. Zhang, Y.-J. Kim, J. Geck, D. G. Hawthorn. "Nematicity in stripe-ordered cuprates probed via resonant x-ray scattering". *Science* **351** (2016), 576–578.

[80] W. Tabis, Y. Li, M. Le Tacon, L. Braicovich, A. Kreyssig, M. Minola, G Dellea, E. Weschke, M. J. Veit, M. Ramazanoglu, A. I. Goldman, T. Schmitt, G. Ghiringhelli, N. Barišić, M. K. Chan, C. J. Dorow, G. Yu, X. Zhao, B Keimer, M. Greven. "Charge order and its connection with Fermi-liquid charge transport in a pristine high-Tc cuprate". *Nat. Commun.* **5** (2014), 5875.

[81] R. Comin, A. Frano, M. M. Yee, Y. Yoshida, H. Eisaki, E. Schierle, E. Weschke, R. Sutarto, F. He, A. Soumyanarayanan, Yang He, M. Le Tacon, I. S. Elfimov, Jennifer E. Hoffman, G. A. Sawatzky, B. Keimer, A. Damascelli. "Charge Order Driven by Fermi-Arc Instability in Bi2Sr2-xLaxCuO6+". *Science* **343** (2014), 390–392.

[82] Eduardo H. da Silva Neto, Pegor Aynajian, Alex Frano, Riccardo Comin, Enrico Schierle, Eugen Weschke, András Gyenis, Jinsheng Wen, John Schneeloch, Zhijun Xu, Shimpei Ono, Genda Gu, Mathieu Le Tacon, Ali Yazdani. "Ubiquitous Interplay Between Charge Ordering and High-Temperature Superconductivity in Cuprates". *Science* **343** (2014), 393–396.

[83] R. Comin, R. Sutarto, E. H. da Silva Neto, L. Chauviere, R. Liang, W. N. Hardy, D. A. Bonn, F. He, G. A. Sawatzky, A. Damascelli. "Broken translational and rotational symmetry via charge stripe order in underdoped YBa2Cu3O6+y". *Science* **347** (2015), 1335–1339.

[84] J. Chang, E. Blackburn, A. T. Holmes, N. B Christensen, J. Larsen, J. Mesot, R. Liang, D. A. Bonn, W. N. Hardy, A. Watenphul, M. v. Zimmermann, M. V. Forgan, S. M. Hayden. "Direct observation of competition between superconductivity and charge density wave order in YBa2Cu3O6.67". *Nture Physics* **8** (2012), 871–876.

[85] Motoaki Hirayama, Youhei Yamaji, Takahiro Misawa, Masatoshi Imada. "Ab initio effective Hamiltonians for cuprate superconductors". *Phys. Rev. B* **98** (2018), 134501.

[86] Peter Fulde, Richard A. Ferrell. "Superconductivity in a Strong Spin-Exchange Field". *Phys. Rev.* **135** (1964), A550–A563.

[87] A. I. Larkin, Y. N. Ovchinnikov. "Nonuniform state of superconductors". *Sov. Phys. JETP* **20** (1965), 762.

[88] A. Buzdin. "Non-uniform Fulde–Ferrell–Larkin–Ovchinnikov (FFLO) state Author links open overlay panel". *Physica B* **407** (2012), 1912.

[89] M. M. Maśka, M. Mierzejewski, J. Kaczmarczyk, J. Spałek. "Superconducting Bardeen-Cooper-Schrieffer versus Fulde-Ferrell-Larkin-Ovchinnikov states of heavy quasiparticles with spin-dependent masses and Kondo-type pairing". *Phys. Rev. B* **82** (2010), 054509.

5 Other scientific achievements

5.1 Before obtaining the PhD degree

The research carried out before obtaining the PhD degree focused on the theoretical analysis of unconventional spin-triplet superconductivity together with its coexistence with magnetism. The materials in which triplet pairing is believed to appear are UGe_2, UIr, URhGe, UCoGe, UNi_2 Al_3, as well as Sr_2 RuO_4. Compounds from this group should be classified as moderately or strongly electron correlated, and in many of them also magnetic ordering appears. We have carried out the analysis of the spin-triplet pairing mechanism induced by the Hund's rule in a two-band Hubbard model. This approach allows for a uniform description of both the superconducting and magnetic phases.

The phase diagrams calculated with the use of the Hartree-Fock approximation, contained the stability regions of both the spin-triplet superconducting phase and superconductivity coexisting with antiferromagnetism and ferromagnetism [1, 2, 3, 4]. As shown, the ferromagnetic ordering can be stable below the Stoner threshold when coexisting with superconductivity. Additionally, enhancement of the superconducting gap is reported in the region for which the ferromagnetic phase begins to stabilize. These two effects show that A1 type spin-triplet pairing and the ferromagnetic ordering support one another. At the next stage of the research, the influence of electron correlation on the considered phenomena has been analyzed with the use of the so-called statistically consistent Gutzwiller (SGA) approximation [5, 6, 7]. The main difference resulting from the electron correlations included within the SGA method was observed for the so-called purely repulsive interactions regime ($U' > J$) [6]. Namely, in this regime the SC phase appeared as stable within the SGA approach, which was not reported earlier for the case of the HF calculations. In such situation the spin-triplet paired state is stabilized by the combined effect of Hund's rule and correlations

[1] M. Zegrodnik, J. Spałek. "Coexistence of spin-triplet superconductivity with antiferromagnetism in orbitally degenerate system: Hartree-Fock approximation". *Acta Phys. Polon.* **121** (2012), 801.

[2] M. Zegrodnik, J. Spałek. "Spin-Triplet Pairing Induced by Hund's Rule Exchange in Orbitally Degenerate Systems: Hartree—Fock Approximation". *Acta Phys. Polon. A* **121** (2012), 1051.

[3] M. Zegrodnik, J. Spałek. "Coexistence of spin-triplet superconductivity with magnetic ordering in an orbitally degenerate system: Hartree-Fock-BCS approximation revisited". *Phys. Rev. B* **86** (2012), 014505.

[4] M. Zegrodnik. "Hund's rule induced spin-triplet superconductivity coexsiting with magnetic ordering in the degenerate band Hubbard model". *Proceedings of the ISD Workshops, Facoulty of Physics and Applied Computer Science, AGH, Kraków. ISBN: 978-83-925779-3-5* (2013).

[5] M. Zegrodnik, J. Spałek, J. Bünemann. "Coexistence of spin-triplet superconductivity with magnetism within a single mechanism for orbitally degenerate correlated electrons: statistically consistent Gutzwiller approximation". *New J. Phys.* **15** (2013), 073050.

[6] M. Zegrodnik, J. Bünemann, J Spałek. "Even-parity spin-triplet pairing by purely repulsive interactions for orbitally degenerate correlated fermions". *New J. Phys.* **16** (2014), 033001.

[7] Spałek, M. Zegrodnik. "Spin-triplet paired state induced by Hund's rule coupling and correlations: a fully statistically consistent Gutzwiller approach". *J. Phys. Condens. Matter* **25** (2013), 435601.

5.2 After obtaining the PhD degree

In the paper [1] the theoretical research on superconductivity in metallic nanostructures was carried out. In particular, it was shown that for the superconducting nanofilms, the quantum effects resulting from electron confinement in the direction perpendicular to the plane of the layer, the value of the critical field may not fulfill the Clogstone-Chandrasekhar relation. In paper [2] the influence of orbital effects on the value of the critical field for superconducting nanofilms was also examined. As shown, the orbital effect decreases the value of critical field and reduces the amplitude of the critical field oscillation as a function of the layer thickness. Moreover, the determined slope of the H_c (T_C) in T_C (0) is in accordance with the available experimental data.

In the paper [3], the possibility of creating the Fulde-Ferrell-Larkin-Ovchinnikov phase in metallic nanofilms was analyzed in the presence of external magnetic field. In particular, as shown by the multiband effects resulting from electron confinement in the direction perpendicular to the layer, the FFLO phase stability region is separated into a series of smaller areas. Each of them corresponds to adjusting the Cooper-pair center-of-mass momentum in order to compensate the mismatch of the Fermi surface from a different band. The possibility of inducing the Fulde-Ferrell phase by orbital effects in nanowires in the external magnetic field was also analyzed [4]. Moreover, in the paper [5] the transport properties of HM/CM/SC heterostructures (semimetal/conical magnet/superconductor) were analyzed as part of a self-consistent approach based on the combination of BTK formalism with BdG equations.

In the paper [6], an alternative approach to the method based on the diagrammatic expansion of the Gutzwiller wave function was presented, in which the diagrammatic summation procedure was carried put in the reciprocal space. Such approach allows to accurately reach the thermodynamic limit. The method was used to analyze the principal models used to describe the strongly correlated fermionic systems. As a result, a good agreement with the experiment was obtained regarding the two Fermi velocities in the copper-based compounds.

In the paper [7], the twisted bilayer graphene system has been analyzed theoretically with the use of an effective two-band model. Within the theoretical approach it was possible to reconstruct the two-dome structure of the superconducting phase reported in the experiment. The topological properties of the considered superconducting phase were also investigated.

[1] P. Wójcik, M. Zegrodnik. "Quantum size effect on the paramagnetic critical field in free-standing superconducting nanofilms". *J. Phys. Condens. Matter* **26** (2014), 455302.

[2] P. Wójcik, M. Zegrodnik. "Orbital effect on the in-plane critical field in free-standing superconducting nanofilms". *Phys. Status Solidi B* **252** (2015), 2096–2103.

[3] P. Wójcik, M. Zegrodnik. "Interplay between quantum confinement and Fulde–Ferrell–Larkin–Ovchinnikov phase in superconducting nanofilms". *Physica E* **83** (2016), 442.

[4] P. Wójcik, M. Zegrodnik, J. Spałek. "Fulde-Ferrell state induced by the orbital effect in a superconducting nanowire". *Phys. Rev. B* **91** (2015), 224511.

[5] P. Wójcik, M. Zegrodnik. "Tunneling conductance through the half-metal/conical magnet/superconductor junctions in the adiabatic and non-adiabatic regimes: Self-consistent calculations". *Physica E* **83** (2016), 466.

[6] M. Fidrysiak, M. Zegrodnik, J. Spałek. "Realistic estimates of superconducting properties for the cuprates: reciprocal-space diagrammatic expansion combined with variational approach". *J. Phys. Condens. Matter* **30** (2018), 475602.

[7] M. Fidrysiak, M. Zegrodnik, J. Spałek. "Unconventional topological superconductivity and phase diagram for an effective two-orbital model as applied to twisted bilayer graphene". *Phys. Rev. B* **98** (2018), 085436.

Mikołaj Zegrodnik